Partitioning net ecosystem carbon exchange into net assimilation and respiration using 13CO2 measurements: a cost-effective sampling strategy

Jérôme Ogée, Philippe Peylin, Philippe Ciais, Thierry Bariac, Yves Brunet, Paul Berbigier, C. Roche, P. Richard, Gérard Bardoux, Jean-Marc Bonnefond

Partitioning net ecosystem carbon exchange into net assimilation and respiration using $^{13}CO_2$ measurements: A cost-effective sampling strategy

J. Ogée,[1] P. Peylin,[2] P. Ciais,[1] T. Bariac,[2] Y. Brunet,[3] P. Berbigier,[3] C. Roche,[2] P. Richard,[2] G. Bardoux,[2] and J.-M. Bonnefond[3]

Received 27 September 2002; revised 28 January 2003; accepted 3 March 2003; published 20 June 2003.

[1] The current emphasis on global climate studies has led the scientific community to set up a number of sites for measuring the long-term biosphere-atmosphere net CO_2 exchange (net ecosystem exchange, NEE). Partitioning this flux into its elementary components, net assimilation (F_A), and respiration (F_R), remains necessary in order to get a better understanding of biosphere functioning and design better surface exchange models. Noting that F_R and F_A have different isotopic signatures, we evaluate the potential of isotopic $^{13}CO_2$ measurements in the air (combined with CO_2 flux and concentration measurements) to partition NEE into F_R and F_A on a routine basis. The study is conducted at a temperate coniferous forest where intensive isotopic measurements in air, soil, and biomass were performed in summer 1997. The multilayer soil-vegetation-atmosphere transfer model MuSICA is adapted to compute $^{13}CO_2$ flux and concentration profiles. Using MuSICA as a "perfect" simulator and taking advantage of the very dense spatiotemporal resolution of the isotopic data set (341 flasks over a 24-hour period) enable us to test each hypothesis and estimate the performance of the method. The partitioning works better in midafternoon when isotopic disequilibrium is strong. With only 15 flasks, i.e., two $^{13}CO_2$ nighttime profiles (to estimate the isotopic signature of F_R) and five daytime measurements (to perform the partitioning) we get mean daily estimates of F_R and F_A that agree with the model within 15–20%. However, knowledge of the mesophyll conductance seems crucial and may be a limitation to the method. *INDEX TERMS:* 0315 Atmospheric Composition and Structure: Biosphere/atmosphere interactions; 1615 Global Change: Biogeochemical processes (4805); 4805 Oceanography: Biological and Chemical: Biogeochemical cycles (1615); *KEYWORDS:* global change, carbon cycle, carbon isotopes, biosphere/atmosphere interactions, forest

Citation: Ogée, J., P. Peylin, P. Ciais, T. Bariac, Y. Brunet, P. Berbigier, C. Roche, P. Richard, G. Bardoux, and J.-M. Bonnefond, Partitioning net ecosystem carbon exchange into net assimilation and respiration using $^{13}CO_2$ measurements: A cost-effective sampling strategy, *Global Biogeochem. Cycles*, *17*(2), 1070, doi:10.1029/2002GB001995, 2003.

1. Introduction

[2] Terrestrial ecosystems are a major component of the climate system through the exchange of energy, momentum, and trace gases with the atmosphere. The spatial and temporal variations of these exchanges are difficult to assess because they involve several physical and biological processes acting at different scales. This is true, in particular, for CO_2 exchange.

[3] In the absence of human activity net CO_2 exchange between terrestrial ecosystems and the atmosphere (net ecosystem exchange, NEE) is the result of carbon uptake during photosynthesis (gross primary production, GPP) and carbon losses during respiration (total ecosystem respiration, TER). TER is a composite flux, involving respiration by foliage, stem, and roots (autotrophic respiration), and respiration by soil organisms (heterotrophic respiration).

[4] A range of multiscale research tools is required to improve our understanding of ecosystem functioning [*Canadell et al.*, 2000; *Running et al.*, 1999]. The net CO_2 flux is now measured continuously at more than 100 continental sites within the world wide network FluxNet using the eddy-covariance technique [*Aubinet et al.*, 2000; *Baldocchi et al.*, 2001]. Combined with CO_2 storage measurements this leads to accurate estimates of NEE at an hourly timescale, at least during daytime periods (see below). However, partitioning NEE into its components GPP and

[1]Laboratoire des Sciences du Climat et de l'Environnement, Commissariat à l'Energie Atomique-Saclay, Gif/Yvette Cedex, France.
[2]Laboratoire de Biogéochimie Isotopique, Centre National de la Recherche Scientifique, Institut National de la Recherche Agronomique, Université Pierre et Marie Curie, Paris, France.
[3]Bioclimatologie, Institut National de la Recherche Agronomique-Bordeaux, Villenave d'Ornon, France.

0886-6236/03/2002GB001995

TER remains necessary to understand the spatial and temporal variations in this exchange [*Janssens et al.*, 2001; *Valentini et al.*, 2000]. The difficulty is that NEE is typically an order of magnitude smaller than these two nearly offsetting terms.

[5] The most straightforward way to estimate TER consists in making leaf, stem, and soil chamber measurements, and scaling them up to the ecosystem level [e.g., *Goulden et al.*, 1996; *Granier et al.*, 2000; *Lavigne et al.*, 1997]. However, this time expensive method requires a heavy experimental setup that cannot be installed routinely at all FluxNet sites. A simple commonly used approach to estimate TER is based on regressions of nocturnal NEE versus soil or air temperature measurements [e.g., *Janssens et al.*, 2001; *Valentini et al.*, 2000]. One difficulty is to get accurate eddy flux measurements during nighttime periods. Indeed, at night, the atmosphere is often stratified and turbulence is sporadic so that other forms of transport, not captured by the eddy-covariance technique (e.g., advection), may become more important. This can lead to an underestimation of TER of up to 30% [*Goulden et al.*, 1996; *Lavigne et al.*, 1997]. In addition, daytime TER is likely to differ from nighttime TER because of light-induced inhibition of leaf respiration [*Brooks and Farquhar*, 1985; *Villar et al.*, 1995]. Extrapolating the regressions found on nocturnal data to daytime periods can therefore lead to an overestimation of TER of up to 15% [*Janssens et al.*, 2001]. Alternate methods to partition NEE into GPP and TER that can be easily applied at the various FluxNet sites must be found in order to reduce the uncertainties on these two terms.

[6] Following an idea of *Yakir and Wang* [1996], *Bowling et al.* [2001] suggested a method to partition NEE into net assimilation F_A ($|F_A|$ = |GPP| – daytime foliar respiration) and nonfoliar respiration F_R (F_R = TER – foliar respiration if daytime) by combining eddy flux measurements and $^{13}CO_2/CO_2$ ratio measurements (hereafter referred to as the EC/flask method). Plants assimilate preferentially the light isotope of CO_2 during photosynthesis, leaving the atmosphere enriched in ^{13}C relative to plant biomass. Since there is apparently no fractionation associated with respiration [e.g., *Lin and Ehleringer*, 1997], the respired CO_2 has the isotopic composition of soil and plant biomass (or assimilates) and is therefore depleted in ^{13}C relative to the atmosphere. Thus a diurnal cycle is apparent in the isotopic composition of air CO_2 that seems to contain enough additional information to allow the partitioning of NEE into F_A and F_R. However, a simple model for canopy conductance is needed to estimate the total ecosystem fractionation associated with net photosynthesis. This requirement is responsible to a large extent for the limitations of the method [*Bowling et al.*, 2001].

[7] The objective of the present paper is to investigate the applicability of this method on a routine basis, i.e., by collecting less isotopic measurements at each campaign, but more regularly during one growing season. To answer this question we first apply the EC/flask method of *Bowling et al.* [2001] at a coniferous temperate forest site that was subject to intensive isotopic measurements in the air, the soil, and the biomass in summer 1997, and test its ability to estimate F_A and F_R. We also adapt the multilayer soil-vegetation-atmosphere transfer model MuSICA [*Ogée et al.*, 2003] to compute flux and concentration profiles of $^{13}CO_2$. Using the model as a "perfect" simulator, and taking advantage of the very dense temporal and spatial resolution of the isotopic data, it is possible to understand how each hypothesis underlying the EC/flask method affects the value of F_A and F_R. Next, we study the impact of retaining only a subset of the isotopic data on the retrieval of F_A and F_R, from which we formulate an efficient and cost-effective sampling strategy.

2. Theoretical Background

[8] In this section we briefly recall the equations used by *Bowling et al.* [2001] to partition NEE into F_A and F_R. For clarity the same notations and conventions are used, except for the storage terms for which the notation seemed misleading.

[9] Conservation of mass for total CO_2 is given by *Raupach* [2001]:

$$\int_0^{z_r} \rho \frac{\partial C_a}{\partial t} dz = \int_0^{z_r} \left(\frac{\partial F}{\partial z} - S \right) dz, \tag{1a}$$

where ρ is the air molar density (mol m^{-3}), C_a (mol mol^{-1}) is the CO_2 concentration at height z and time t, F (mol m^{-2} s^{-1}) and S (mol m^{-3} s^{-1}) are the CO_2 flux and source density (at level z and time t), and z_r is a reference height above the vegetation. Equation (1a) can be rewritten as:

$$\rho \left\langle \frac{dC_a}{dt} \right\rangle = \rho \overline{w' C_a'} - (F_A + F_R), \tag{1b}$$

where $\rho \overline{w' C_a'}$ is the net CO_2 flux above vegetation (measured by eddy-covariance at level z_r, the over bar denoting Reynolds averaging and the primes denoting fluctuations from this average) and $\rho \langle dC_a/dt \rangle$ is the CO_2 air storage between the ground and the level above vegetation at which the net CO_2 flux is measured. By convention upward scalar fluxes are positive.

[10] Conservation of mass for $^{13}CO_2$ is given by:

$$\rho \left\langle \frac{dC_a R_a}{dt} \right\rangle = \rho \overline{w' (C_a R_a)'} - \left(\frac{R_a}{1 + \Delta_A} F_A + R_r F_R \right), \tag{2}$$

where Δ_A is the fractionation factor associated with net photosynthesis, and R_r and R_a refer to the $^{13}CO_2/CO_2$ ratios in canopy air and respired CO_2. Rewriting this equation in δ notation ($\delta = R/R_{PDB} - 1$, where R_{PDB} is the isotope ratio of the Pee Dee Belemnite standard) gives:

$$\rho \left\langle \frac{dC_a \delta_a}{dt} \right\rangle = \rho \overline{w' (C_a \delta_a)'} - (\delta_a - \Delta_A) F_A - \delta_r F_R, \tag{3}$$

where $\rho \overline{w' (C_a \delta_a)'}$ is the so-called eddy isoflux [*Bowling et al.*, 2001] and $\rho \langle dC_a \delta_a / dt \rangle$ is the isostorage, i.e., the $^{13}CO_2$ air storage in δ units. Equations (1) and (3) can then be rewritten as:

$$F_A + F_R = \text{eddy flux} + \text{storage}, \tag{4a}$$

$$(\delta_a - \Delta_A) F_A + \delta_r F_R = \text{eddy isoflux} + \text{isostorage}. \tag{4b}$$

[11] Equations (4a) and (4b) can be seen as a system of two equations with two unknowns (F_A and F_R). To solve this system in F_A and F_R we need to know all other variables, i.e., storage, isostorage, eddy flux, eddy isoflux, δ_r, δ_a, and Δ_A.

[12] The eddy flux is measured by eddy-covariance at a reference level z_r above vegetation. The storage and isostorage terms are computed from air CO_2 concentration and $^{13}CO_2/CO_2$ ratio measurements at different heights between the ground and the level where the eddy flux is measured. *Bowling et al.* [2001] computed the eddy isoflux by expressing δ_a as a linear combination of C_a during daytime and using this relationship to retrieve a 10-Hz time series for δ_a:

$$\overline{\rho w'(C_a\delta_a)'} = \overline{\rho w'(C_a(mC_a+p))'} = \left(2m\overline{C_a}+p\right)\overline{\rho w' C_a'} + m\overline{\rho w' C_a' C_a'}. \quad (5)$$

[13] They verified empirically that such a linear relationship between δ_a and C_a holds from a variety of timescales (500 ms, 30 s, and 30 min).

[14] The fractionation associated with net photosynthesis Δ_A is computed according to *Farquhar et al.* [1989]:

$$\Delta_A = \bar{a} + (b-\bar{a})\frac{C_c}{C_a}, \quad (6)$$

where $\bar{a}$ is the fractionation resulting from the diffusion of CO_2 between the canopy air space and the sites of carboxylation, b is the net fractionation of the enzyme-catalyzed fixation of CO_2 [≈27‰, *Farquhar et al.*, 1989; *Farquhar and Lloyd*, 1993], and C_c is the CO_2 concentration at the carboxylation sites. Neglecting the resistance for CO_2 diffusion from the stomatal cavity to the mesophyll wall with respect to the stomatal resistance leads to [*Farquhar et al.*, 1989; *Farquhar and Lloyd*, 1993]:

$$\bar{a} = \frac{a_b g_c + a g_a + (a_s(T)+a_1) g_c g_a r_m}{g_c + g_a + g_c g_a r_m} \text{ with } \frac{1}{g_a} = \frac{1}{g_t} + \frac{1}{g_b}, \quad (7)$$

where g_c is the bulk canopy conductance for CO_2 (the stomatal conductance at the leaf scale, see equation (9) below), g_a is the aerodynamic conductance for CO_2 diffusion in air, r_m is the resistance to CO_2 diffusion within the mesophyll, a_b is the fractionation associated with diffusion in the laminar boundary layer (2.9‰), a is the fractionation due to molecular diffusion from the leaf surface to the substomatal cavity (4.4‰), $a_s(T)$ is the fractionation as CO_2 enters solution (1.1‰ at 25°C), and a_1 is the fractionation caused by diffusion within the cell (0.7‰). The aerodynamic resistance $1/g_a$ is expressed as the sum of a turbulent resistance $1/g_t$ and a boundary layer resistance $1/g_b$ [*Lamaud et al.*, 1994]. The value of $\bar{a}$ varies between about 3.6‰ (in the morning when g_c takes its maximum value) and a = 4.4‰ (during the night when $g_c = 0$).

[15] Equation (7) was obtained by using the standard "big leaf" multiple resistance model. In this framework, C_c is given by:

$$-F_A = \frac{g_c g_a}{g_c + g_a + g_c g_a r_m}(C_a - C_c). \quad (8)$$

[16] The bulk canopy conductance g_c is given by the Penmann-Monteith equation:

$$\frac{1}{1.6g_c} = \frac{s(R_n - \mathrm{LE} - G)/g_a'' + \rho c_p D_a}{\gamma \mathrm{LE}} - \frac{1}{g_a'}, \quad (9)$$

where s (kg kg^{-1} K^{-1}) is the slope of the saturation vapor pressure versus temperature curve, R_n, LE, and G (W m^{-2}) are net radiation, latent, and storage heat fluxes, respectively, c_p (J kg^{-1} K^{-1}) is the specific heat of air, D_a (kg kg^{-1}) is the air saturation vapor deficit, and $\gamma = c_p/L$ (K^{-1}) is the psychrometric constant. The 1.6 factor arises in the conversion from conductance for CO_2 to H_2O.

[17] The conductances g_a' and g_a'' are the counterparts of g_a for water vapor and sensible heat, respectively, and are given by:

$$\frac{1}{g_a'} = \frac{1}{g_t} + \frac{1}{1.4g_b} \quad \text{and} \quad \frac{1}{g_a''} = \frac{1}{g_t} + \frac{1}{1.4 \times 0.92 g_b}. \quad (10)$$

[18] The 1.4 and 0.92 factors arise from the conversion of conductances for CO_2 to conductances for H_2O or sensible heat.

[19] We use here the following expressions for g_t and g_b [*Lamaud et al.*, 1994]:

$$g_t = U_*^2/U_r \quad \text{and} \quad g_b = U_* B (Sc/Pr)^{-2/3}. \quad (11)$$

[20] The expression for g_t uses the friction velocity U_*, i.e., the square root of the momentum flux at the reference level above vegetation, and the mean wind speed U_r at the same height. This expression is true for stable and near-neutral conditions but in unstable conditions this amounts to neglecting the differences in stability corrections between momentum and scalars. However, this approximation turns out to be much better than trying to evaluate g_t from surface layer log law, since our measurement level is well within the roughness sublayer. The expression for g_b makes use of the inverse Stanton number ($B \approx 1/7.5$, as given by *Lamaud et al.* [1994] at the same site), the Schmidt number for CO_2 (Sc = 1.02) and the turbulent Prandtl number (Pr = 0.72), so that it reduces to $g_b \approx U_*/10$.

[21] The EC/flask method can be decomposed into several steps (Figure 1). Nighttime air isotopic data are needed to determine δ_r (see below), while daytime data are used to estimate both the eddy isoflux (equation (5)) and the isostorage. The Penmann-Monteith equation is used to estimate the bulk canopy conductance and Δ_A. Finally, from equations (4a) and (4b) we can retrieve F_R and F_A. The assumptions underlying each of these steps are critically analyzed and tested in what follows.

3. Materials and Methods

3.1. Research Area

[22] The experimental site is located at about 20 km from Bordeaux, France (44°43′N, 0°46′W, altitude 62 m) in a nearly homogeneous maritime pine stand (*Pinus pinaster* Ait.) planted in 1970. The trees are distributed in parallel rows along a NE-SW axis with an interrow distance of 4 m. In September 1997 (period at which the isotopic measurements were performed), the stand density was 520 trees per

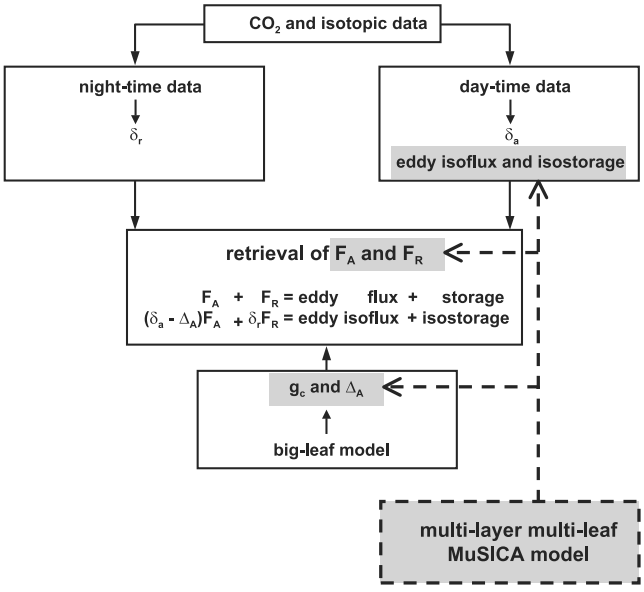

Figure 1. Diagram showing the different steps necessary to retrieve F_A and F_R fluxes from equations (4a) and (4b). In this study the multilayer multileaf MuSICA model is used to check the values of (1) the eddy isoflux and the isostorage, (2) the bulk photosynthesis discrimination factors and the associated canopy conductance, and (3) F_A and F_R.

hectare; the mean tree height was about 18 m and the projected leaf area index was around 3. The canopy is confined to the top 6 m [*Porté et al.*, 2000] so that canopy and understorey constitute two separate layers. The latter is mainly made of grass (*Molinia coerulea*) whose roots and stumps remain throughout the year but whose leaves are green only from April to late November, with maximum leaf area index and height of 1.4–2.0 and 0.6–0.8 m, respectively [*Loustau and Cochard*, 1991; *Ogée et al.*, 2003]. A 5-cm thick litter made of compacted grass and dead needles is present all yearlong. The water table never goes deeper than about 200 cm. In September 1997, soil water content in the top 80 cm went down to 60 mm so that the effect of water stress on CO_2 and water vapor exchanges was noticeable [*Ogée et al.*, 2003].

3.2. Flux and Meteorological Measurements

[23] The experimental setup that provided the flux and meteorological measurements used here was installed following the requirements of EUROFLUX (the European network in FluxNet). At 25 m above ground, considered here as our reference level z_r, the following data were measured every 10 s and averaged every 30 min: net radiation with a Q7 net radiometer (REBS, Seattle, WA); incident solar radiation with a C180 pyranometer (Cimel, France); air temperature and specific humidity with a 50Y temperature-humidity probe (Vaisala, Finland). Wind speed, friction velocity, and sensible heat flux were measured with a 3D sonic anemometer (Solent R2, Gill Instruments, Lymington, Hampshire, UK), and water vapor and carbon dioxide fluxes were computed using the sonic anemometer coupled with an infrared gas analyzer (LI-6262, LICOR, Lincoln, NE, USA). Rainfall was measured at 20 m with an ARG100 rain gauge (Young, USA). All additional details can be found in the work of *Berbigier et al.* [2001].

3.3. Air CO_2 Measurements

[24] Ambient air samples from 11 heights (0.01, 0.2, 0.7, 1, 2, 6, 10, 14, 18, 25, and 38 m) were pumped continuously during a 2-month period starting on 4 September 1997. The pump was coupled with an electrovalve to scan the various levels every 2–3 min and a second infrared gas analyzer (LI-6262, LICOR, Lincoln, NE) was used (in the absolute mode) for CO_2 analysis. Half-hour time series were then computed by linear interpolation. The overall precision of air CO_2 measurements was estimated at ±10 ppmv, which includes both measurement and sampling errors.

3.4. Isotope Measurements

[25] All isotopic measurements were made on 4 September (day 247) and the following night.

[26] Ambient air samples from the same 11 levels used for CO_2 sampling were predried by passage through a mixture of ethanol-solid carbon dioxide to remove H_2O and collected every half-hour (night) or every hour (day) into glass flasks for isotopic analysis. A total of 341 flasks were analyzed. The analysis of $\delta^{13}CO_2$ was performed using a gas chromatograph (Hewlett Packard 5890 Series II, Hewlett Packard Co. Ltd) coupled with an isotope ratio mass spectrometer (Optima, Fisons Instruments, Valencia, CA).

[27] Tree collar and foliage (needle and leaf) samples were collected each hour from trees and grass samples near the mast for stable isotope analysis. Tree collar samples were collected by coring the trunks at 0.5 m from ground level with an increment borer. Soil profiles were drilled with an auger at 0.025 m intervals from 0 to 0.05 m below the surface and at 0.05 m intervals from 0.05 to 0.5 m.

[28] Total organic material was dried in a vacuum line at 60°C. Dried material was crumbled into a fine powder (<100 mm) and carefully homogenized and combusted in an elemental analyzer (CHN-type, NA 1500, Fisons Instruments, Valencia, CA, USA). Evolved gases were cryogenically purified and separated in a trapping system with different and variable temperatures, and finally introduced in a gas isotope ratio mass spectrometer (SIRA 10, Fisons Instruments, Valencia, CA, USA) equipped with double inlet system and triple ionic collection.

[29] Carbon isotope ratios are calculated as:

$$\delta^{13}C = R_{sample}/R_{PDB} - 1, \quad (12)$$

where R_{sample} and R_{PDB} are the $^{13}C/^{12}C$ ratios of the sample and the Pee Dee Belemnite standard, respectively. The overall precision of the carbon isotope measurements is ±0.3‰.

3.5. MuSICA Model

[30] The MuSICA model is a multilayer multileaf biophysical soil-vegetation-atmosphere transfer model [*Ogée et*

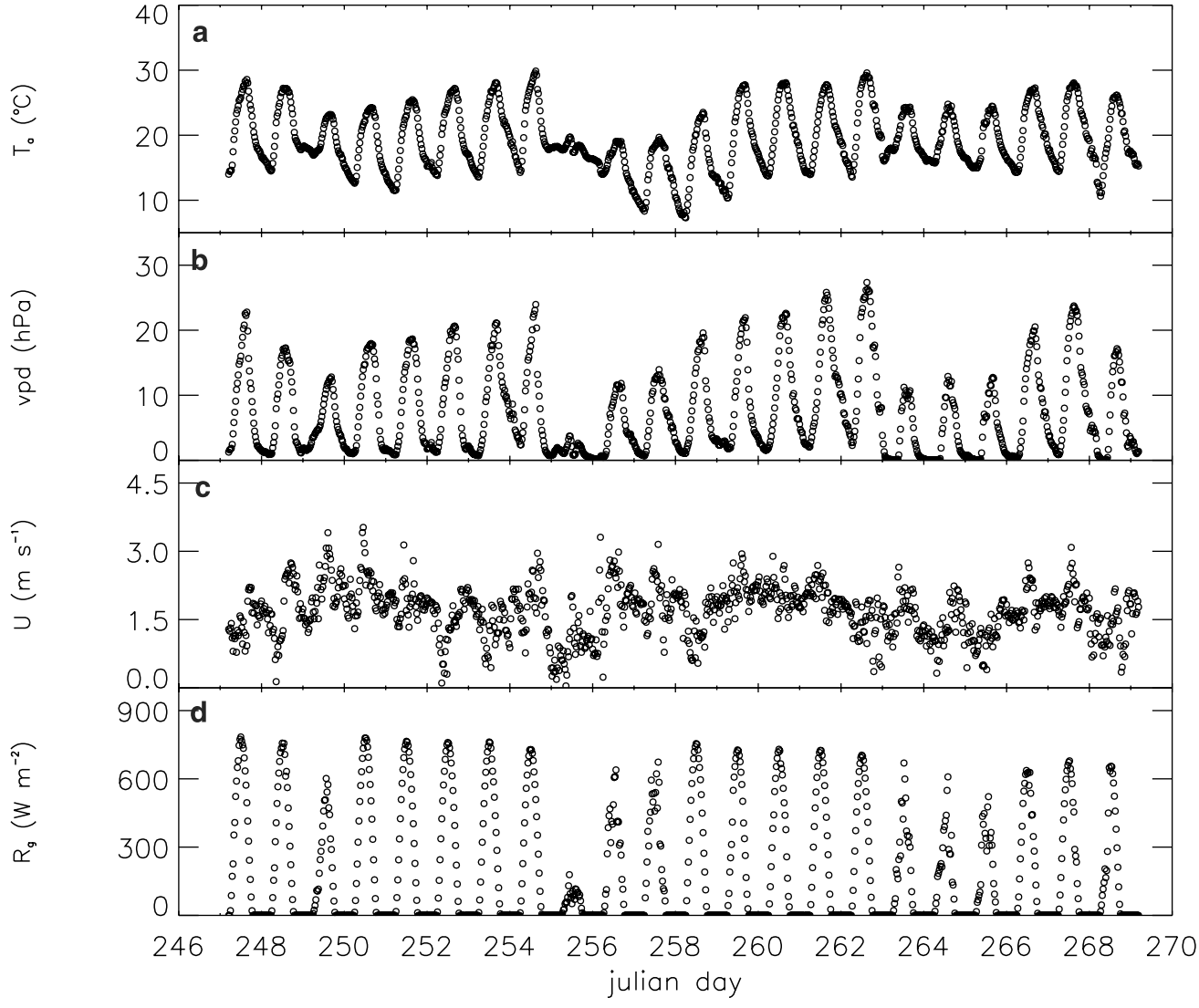

Figure 2. Meteorological data at the Bray site during the 22-day period considered in this study (4–25 September 1997): (a) air temperature, (b) air vapor pressure deficit, (c) wind speed, and (d) global radiation measured at 25 m above ground. Rain occurred only on day 256 and did not exceed 7 mm. See color version of this figure in the HTML.

al., 2003]. Its key features are that (1) in each vegetation layer, the model distinguishes several types of "big leaves" (or "big shoots") according to their age, sun exposure (sunlit or shaded), and water status (wet or dry) and (2) the transport of the different atmospheric scalars (temperature, water vapor, CO_2, ...) is described with a Lagrangian turbulent transfer model [*Raupach*, 1989b], and for different atmospheric stability conditions.

[31] For this study the total number of layers is set to 36 with 30 layers within the vegetation and 3 layers in the understorey (instead of 12, 10, and 1, respectively, of *Ogée et al.* [2003]) in order to better capture the shapes of the scalar profiles within the vegetation. We also added the transport of the $^{13}CO_2$ tracer (see Appendix A). This version of MuSICA is then able to compute air CO_2 and $\delta^{13}CO_2$ profiles, and the various components of the carbon budget, GPP, TER, but also F_A and F_R. It is therefore suitable to test the different assumptions underlying the EC/flask method.

4. Results and Discussion

4.1. Meteorological Conditions

[32] The isotopic measurements were performed during one single 24-hour period. As in the work of *Bowling et al.* [2001], we used these measurements to estimate the three coefficients δ_r, m, and p in equations (4) and (5). Then assuming that these coefficients do not change much over time, we applied the EC/flask method to partition NEE into F_A and F_R on a longer period. On day 269, a strong storm occurred so that we preferred to restrict this analysis to 22 days only. The meteorological variables during this 22-day period (comprising the day of measurements and the following 21 days) are shown in Figure 2. We can see that this

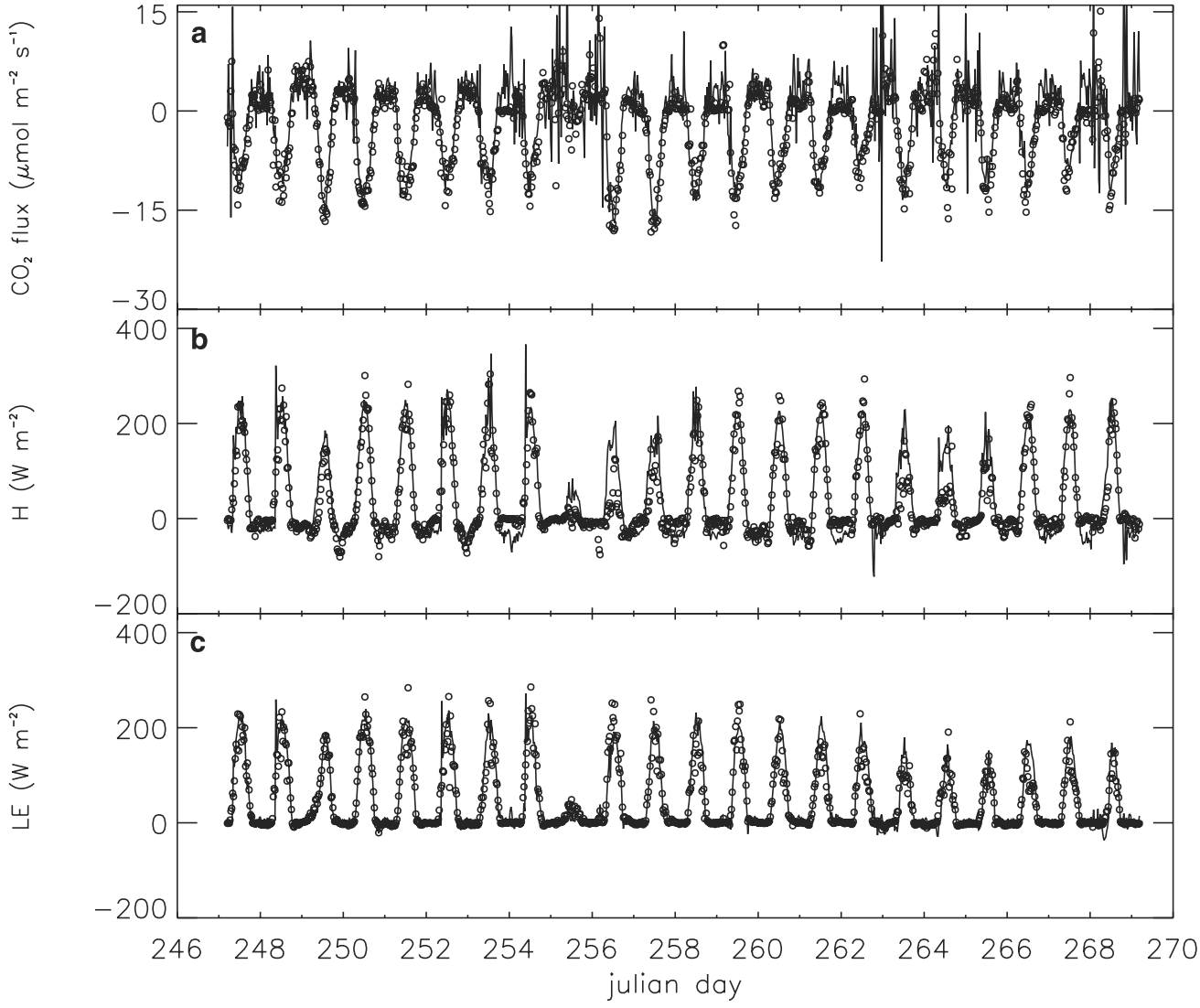

Figure 3. Measured (open circles) and modeled (solid line) fluxes over the 22-day period (4–25 September 1997): (a) CO_2 flux, (b) sensible heat flux, and (c) latent heat flux. See color version of this figure in the HTML.

period includes mostly sunny days with a few cloudy days (249, 255–257, and 263–265), characterized by colder and moister air. It occurred at the end of summer, at a time when the soil water content had fallen below 70 mm and water stress was noticeable on water vapor flux (see below and Figure 3). Only one light rain event occurred on day 255 but the amount of rainwater did not exceed 7 mm. We must notice that the whole period is characterized by a light wind (less than 3 m s^{-1}), especially during the night and in the early morning. This is usually in favor of rapid changes, from stable to unstable, of the atmospheric conditions which are difficult to model correctly and may compromise the model performance (see below).

4.2. Evaluation of the Model Behavior

[33] Figure 3 shows the measured and modeled turbulent fluxes for sensible heat, water vapor, and CO_2 over the 22-day period. Generally, the MuSICA model reproduces correctly the diurnal variations of all fluxes [see also *Ogee et al.*, 2003]. In particular, the effect of cloudiness and water stress on latent heat and CO_2 fluxes seems well accounted for. However, at some specific times the modeled fluxes show rapid temporal variations. This is particularly the case for the CO_2 flux. These rapid variations mostly occur during the night or in the early morning (i.e., when the wind is low), and result from an excessive CO_2 storage term usually followed (the next time step or later) by a flush out of the same order of magnitude.

[34] In MuSICA, scalar profiles are computed iteratively because they depend on the scalar source densities, which in turn depend on the scalar profiles. In addition, the turbulent transport module in MuSICA requires steady turbulence: at each time step a new profile is computed in "equilibrium" with the scalar source densities and without keeping memory of the scalar profile at the previous time step. When wind velocity is low the model does not always converge properly because it can switch from very stable to very

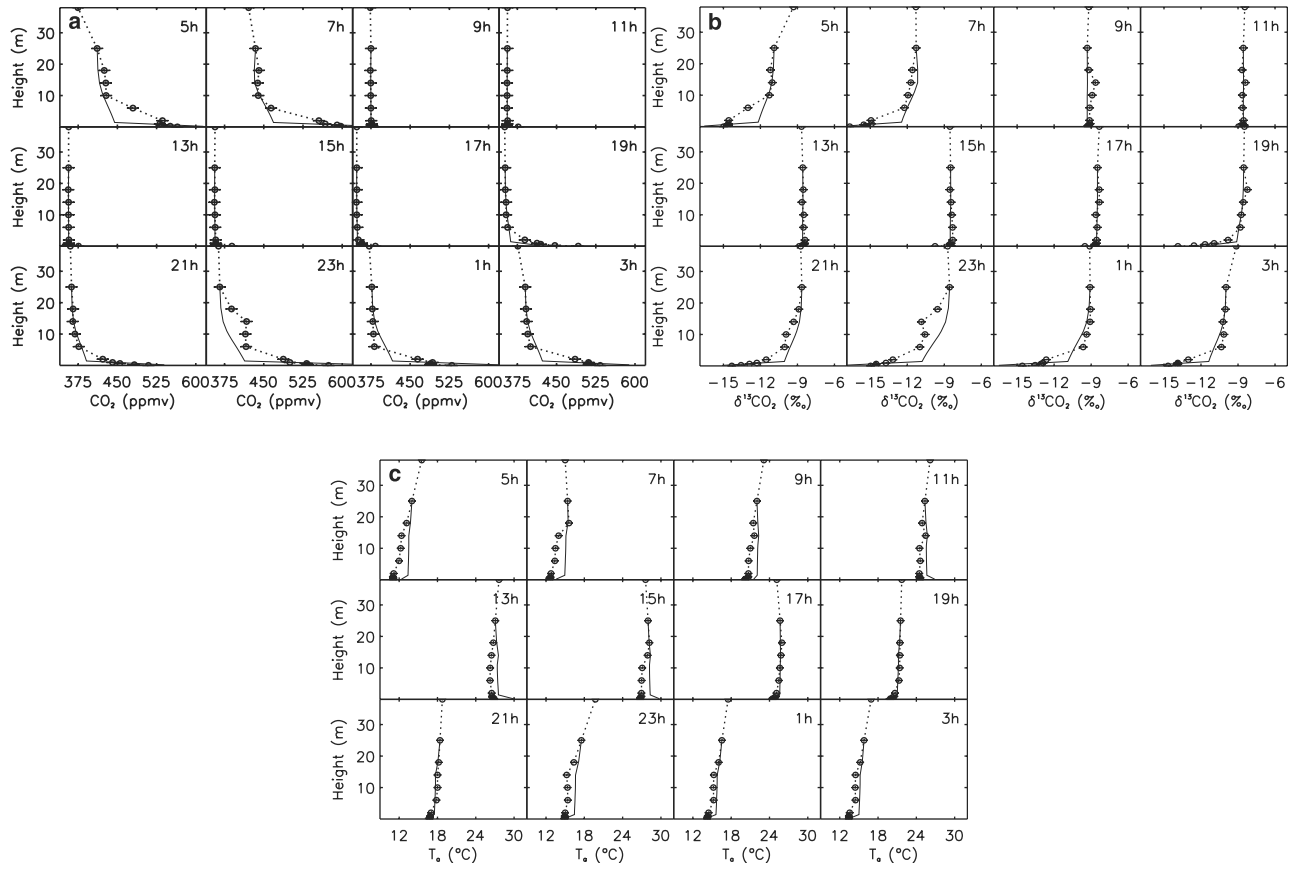

Figure 4. Measured (open circles) and modeled (solid line) profiles at different times of the day on 4 September 1997 and for three different scalars: (a) CO_2, (b) $\delta^{13}CO_2$, and (c) air temperature. Canopy is confined in the 11–17 m region and understorey is below 1 m. Solar time is indicated for each profile. See color version of this figure in the HTML.

unstable conditions, depending on the sign of the sensible heat flux. In such case, the predicted scalar profile is numerically unstable, and combined with the previous scalar profile, it may result in excessive air storage terms. Note that at night, CO_2 concentrations in the understorey are often 150 ppmv larger than at the reference level. A flush out of only 50 ppmv over a 25-m high air column during one time step of 1800 s corresponds to a flux of more than 25 μmol m^{-2} s^{-1}, which is an order of magnitude larger than the nighttime CO_2 flux. This explains why MuSICA can easily predict rapid CO_2 flux variations with wrong but still realistic values of air CO_2 concentrations.

[35] Figures 4a and 4b show the measured and modeled air CO_2 and $\delta^{13}CO_2$ profiles at different times of day 247. It can be seen that the model correctly reproduces the different profiles, but systematically underestimates the CO_2 and $^{13}CO_2$ nighttime gradients above the understorey (between 1 and 6 m). We also notice that the disagreement between model and measurements has always the same tendency for both CO_2 and $\delta^{13}CO_2$ profiles, which indicates a consistency between the two tracers, and between model and measurements. Figure 4c shows the measured and modeled air temperature profiles for the same day. As for CO_2 and $\delta^{13}CO_2$, the disagreement between modeled and measured air temperature is greater at 0500, 0700, and 2300 hours, which indicates a consistency between this tracer and the two others. Inspection of the measured temperature profiles at 0700 hours shows that turbulence is characterized as unstable within and above the canopy, and stable in the understorey. MuSICA, which only uses one turbulent parameter to describe both canopy and understorey turbulence, cannot account for this duality and switches from stable to unstable conditions without converging. At this time of the day the modeled sensible heat flux is dominated by the air storage term. For this reason, we think that the scalar profiles given by MuSICA are acceptable only when air storage in sensible heat is smaller than the sensible heat flux.

4.3. Determination of δ_r

[36] *Bowling et al.* [2001] determined the value of the respired CO_2 signature δ_r using the Keeling model [*Keeling*, 1961]. In this model, the value of δ_r is defined as the intercept of the regression of δ_a versus $1/C_a$ during nighttime. Note that the determination of δ_r requires extrapolation far from the actual range of measurements, possibly leading to large errors and sensitivity to outliers. As an alternative, we determined δ_r as the "instant" slope of the regression between the product $C_a\delta_a$ and C_a, as suggested by *Bakwin et al.* [1998]. We used an orthogonal

Table 1a. Intercept (Respective Slope) of the Regression Between C_a and $1/\delta_a$ (Respective $C_a\delta_a$ and C_a) During the Night (Before 0700 Hours and After 1900 Hours) Using All Levels and All Time Steps or All Levels for Each Time Step[a]

	δ_r, ‰	n	r^2
Keeling (C_a versus $1/\delta_a$) all levels: all time steps	−26.9 ± 0.1	187	0.99
Instant slope ($C_a\delta_a$ versus C_a) all levels: all time steps	−26.8 ± 0.1	187	1.00
All levels: average time step	−27.1 ± 0.3	19	...

[a]In the latter case, only the mean value (over all time steps) and its standard deviation are shown.

distance regression [*Press et al.*, 1992] to account for errors both on δ_a (0.3‰) and C_a (10 ppmv).

[37] During our isotope experiment 187 flasks were collected at nighttime (between about 1900 and 0700 hours). Inspection of the results reported in Table 1a shows that the value of δ_r obtained using the Keeling model is nearly equal to, and statistically as good as, that obtained using the instant slope model. This value (−26.8 ± 0.1‰) is also in close agreement with the measured bulk ^{13}C isotopic composition of the various carbon reservoirs, i.e., soil organic matter and plant biomass (Table 1b).

[38] Two assumptions are at the origin of the Keeling model (or the instant slope model). First, we assume the existence of a ''background'' infinite reservoir of constant isotopic composition during the whole night. Second, we assume that all the respired carbon originates from the same source with unique isotopic composition δ_r.

[39] In order to test the constancy of δ_r during the night, we performed a $C_a\delta_a$ versus C_a regression for each time step. The very dense vertical resolution of the sampling during this campaign made this possible. The results are encouraging as it is not possible to detect any temporal evolution in δ_r. The scatter between all time steps is small (standard deviation of 0.3‰) with a mean value (−27.1‰) close to the value obtained with the full data set (−26.8‰). This seems to indicate that the respired CO_2 keeps a constant isotopic composition over the night.

[40] In order to test the uniqueness of δ_r we also made $C_a\delta_a$ versus C_a regressions for each level. The results in Figure 5a show that the value obtained with the full data set (in gray in the figure) is actually smaller than any value obtained with a subset corresponding to one single level. This indicates that the intercept of the $C_a\delta_a$ versus C_a regression also varies from one level to another because the background reservoir is probably not the same at each level. We also see in Figure 5a that the source of respired $^{13}CO_2$ seems more enriched around 10–15 m and close to the ground than at any other level. Because the canopy layer is located around 11–17 m and the understorey is confined in the first meter above ground, this may indicate that the CO_2 respired by canopy needles and understorey leaves is more enriched than the CO_2 respired by the other sources (trunk, branches, and soil). The bulk ^{13}C isotopic composition of the various organic matter reservoirs (leaves, needles, collar, and soil) have nearly the same value (around −28‰, see Table 1b). This implies that the CO_2 respired by leaf elements has a different isotopic signature than whole-leaf dry matter. Such a situation has already been observed on coniferous needles [*Brendel*, 2001]. Indeed, leaves contain both structural carbon and newly fixed carbon (soluble sugars and starch) that may have a different isotopic composition [e.g., *Le Roux et al.*, 2001]. At a short timescale (less than a day), the isotopic composition of carbon that has been newly fixed by a leaf is well correlated with the C_c/C_a ratio, i.e., the isotopic discrimination of the leaf [*Lauteri et al.*, 1993]. Over night the carbon respired by a leaf is likely to have an isotopic composition closer to that of this newly fixed carbon than that of the whole-leaf dry matter.

[41] We used the MuSICA model to investigate this issue. We plotted in Figure 5b the δ_r values at each level obtained with the C_a and δ_a profiles given by the model. The latter is forced by the C_a and δ_a measurements at 25 m. The δ_r value at this level is not exactly the same in Figures 5a and 5b (−26.3 ± 1.6 and −26.5 ± 1.4‰, respectively) because in order to get continuous forcing variables over the whole night and run the model, we interpolated missing δ_a values at 25 m with the $C_a\delta_a$ versus C_a linear regression used to get δ_r. The plot in Figure 5b was obtained with a constant and unique isotopic composition (fixed at −28‰) for all respiring plant and soil elements accounted for in MuSICA (i.e., 1-, 2-, and 3-year-old needles, trunks, and branches, understorey leaves, roots, and soil heterotrophs). As expected, the δ_r values vary smoothly from the value fixed at 25 m (−26.5‰) and a value close to −28‰ at the ground. They do not reproduce the observed air isotopic enrichment around 10–15 m and close to the ground. We modified the isotopic composition of the various respiring plant and soil elements in MuSICA and tried to retrieve this

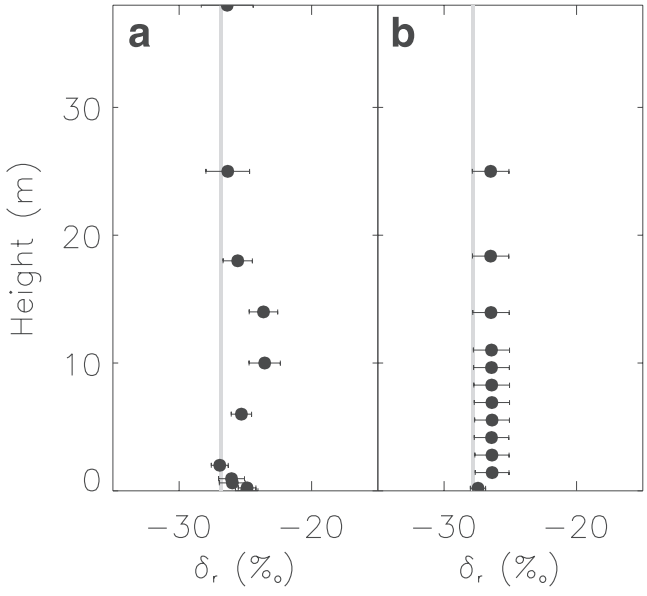

Figure 5. Isotopic signature of respired CO_2 (δ_r) inferred from the slope of the $C_a\delta_a$ versus C_a linear regressions at each level within the canopy using all available nighttime profiles on 4 September 1997 (a) from measurements or (b) from the model where CO_2 respired by all respiring organs is set to the same isotopic composition. Gray lines indicate the average value and the standard deviation obtained when using the full data set (all levels together).

Table 1b. ^{13}C Isotopic Composition of Canopy Needles and Collar, Understorey Leaves and Collar, and Soil Organic Matter at the Bray Site on 4 September 1997

	$\delta^{13}C$, ‰	*n*
Canopy		
Bottom: 0–1 year old needle	−28.7 ± 0.4	11
Bottom: 1–2 year old needle	−27.7 ± 0.3	10
Bottom: 2–3 year old needle	−27.3 ± 0.3	5
Top: 1–2 year old needle	−28.1 ± 0.3	17
Collar	−26.0 ± 0.5	7
Understorey		
Leaves	−29.8 ± 0.5	40
Collar	−28.5 ± 0.7	40
Soil Organic Matter		
	−28.0 ± 0.3	16

air enrichment within the two green vegetation layers. Within a realistic range of $\delta^{13}C$ values (−28 ± 5‰) the model is unable to generate a δ_r profile as in Figure 5a. The model apparently does not match well enough the CO_2 and $\delta^{13}CO_2$ profiles within the vegetation during the night (Figure 4, between 1900 and 0700 hours). At these levels MuSICA apparently predicts too strong air mixing so that the air isotopic composition is not affected enough by the CO_2 respired by leaves or needles. This also explains why the value at the ground is not exactly equal to −28‰. *Warland and Thurtell* [2000] found that the turbulent transfer theory used in MuSICA could lead to an overestimation of the air mixing near the sources. They suggested an alternate model that should be tested in the future.

[42] In equations (4a) and (4b) δ_r represents the isotope signature of daytime nonfoliar respiration. When we estimate δ_r from nighttime profiles we assume that the isotopic signature for foliar and nonfoliar or daytime and nighttime respiration is unique. If foliar respiration at night has a different isotopic signature than nonfoliar respiration it is not quite correct to estimate δ_r from nighttime profiles. Foliar respiration at night represents about 1/3 of total respiration. Because C_a and δ_a measurements above the vegetation integrate all sources of CO_2 below, they should be less affected by foliar respiration than any measurement performed within vegetation layers. The estimation of δ_r should then be performed only from C_a and δ_a measurements taken at levels above the vegetation in order to reduce the possible bias caused by foliar respiration. In what follows, we keep the value of δ_r estimated from all levels (−26.8 ± 0.1‰) because it is close to the value found at levels above the vegetation (25 and 38 m) and has much lower uncertainty due to the larger data set. Other campaigns with the same dense vertical resolution are strongly needed to confirm our results.

4.4. Determination of the Eddy Isoflux

[43] In order to retrieve a 10-Hz time series for δ_a and compute the eddy isoflux (equation (5)), we first need to determine the daytime linear regression between δ_a and C_a at 25 m (where the eddy flux is measured).

[44] *Bowling et al.* [2001] provided no theoretical justification for the existence of a linear relationship between δ_a and C_a but they rather convincingly verified its robustness empirically. In fact, one would expect a linear relationship to hold true only between the product $C_a\delta_a$ and C_a. An observer placed at a given height above the canopy always measures gas concentration from different air parcels, or eddies, which originate from other heights. An arbitrary degree of mixing occurs, but in the absence of sources during the parcel transit, any rapid change detected in gas concentration relates to the vertical concentration gradient and to the parcel origin. In the case of two conservative tracers, here $C_a\delta_a$ and C_a, the ratio of their concentration changes is preserved during mixing, and it is equal to the ratio of the two gradients. It is shown in Appendix B that, under the above conditions, the linear relationship between δ_a and C_a observed by *Bowling et al.* [2001] is a good approximation of an exact linear regression between $C_a\delta_a$ and C_a. It seemed therefore preferable to compute the eddy isoflux from a linear regression of $C_a\delta_a$ and C_a, as was done for nighttime values to find the Keeling plot intercept.

[45] Writing $C_a\delta_a = MC_a + P$ leads to a simpler relationship (compared to equation (5)) between the CO_2 eddy flux and the corresponding eddy isoflux:

$$\rho\overline{w'(C_a\delta_a)'} = \rho\overline{w'(MC_a + P)'} = M\rho\overline{w'C_a'}. \qquad (13)$$

[46] In the case where $M = \delta_r$ (and under the hypothesis that the storage terms can be neglected during the day) we cannot estimate F_A and F_R anymore as equations (4a) and (4b) become proportional and isotopic equilibrium ($\delta_a - \Delta_A = \delta_r$) is reached. Fortunately, isotopic equilibrium is unlikely to be satisfied at an hourly timescale. Indeed, Δ_A (so as g_c) reacts rapidly to plant water status and radiation changes [e.g., *Le Roux et al.*, 2001] while δ_r is a time integrator of $\delta_a - \Delta_A$. It must therefore be possible to use equation (13) to retrieve F_A and F_R.

[47] The values of M and P used in equation (12) were estimated from the CO_2 and $^{13}CO_2$ daytime measurements at 25 m (Table 2). Inspection of the results shows that the slope M used in equation (13) (−23.6‰) is actually far from the equilibrium value (−26.8‰), indicating that the partitioning exercise seems possible.

[48] We only used the measurements at 25 m to determine M and P because it was the level at which the eddy flux was measured. We also computed the slope M of the $C_a\delta_a$ versus C_a linear regression obtained at the other levels (Figure 6). We can see that the air near the ground is more in equilibrium than the air above the vegetation as the value of M gets closer to δ_r with decreasing height. This is due to soil respiration having a greater weight in the total CO_2 source/

Table 2. Slope and Intercept of the Linear Regression Between $C_a\delta_a$ and C_a Using Either the 25-m Level Only or the Four Levels Between 14 and 38 m

	m or *M*	*p* or *P*	*n*	r^2
Bowling (δ_aVersus C_a)				
Reference level	−0.036 ± 0.0021	4.4 ± 0.7	14	0.97
14–38 m levels	−0.038 ± 0.001	5.2 ± 0.4	56	0.97
Instant Slope ($C_a\delta_a$Versus C_a)				
Reference level	−23.6 ± 0.8	(5.4 ± 0.3) × 10^3	14	0.99
14–38 m levels	−24.1 ± 0.4	(5.7 ± 0.1) × 10^3	14	0.99

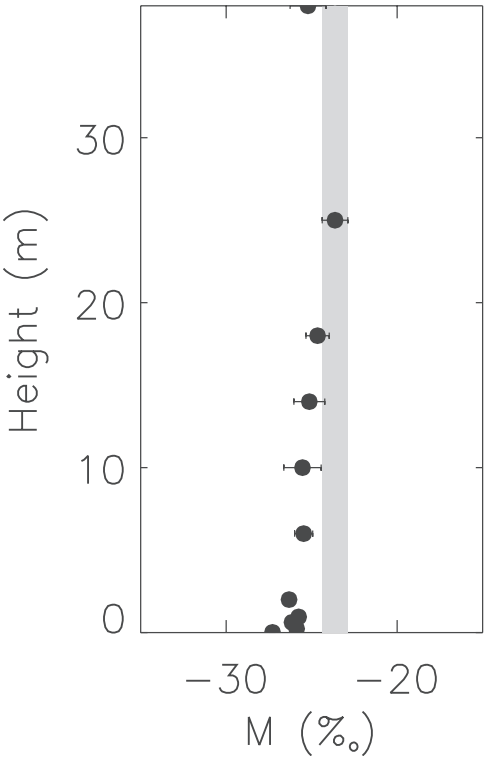

Figure 6. Slope M of $C_a\delta_a$ versus C_a regressions made at each level within the canopy using all available daytime profiles on 4 September 1997. The value obtained at 25 m and used to compute the eddy isoflux and its standard deviation is indicated in gray.

sink strength near the ground. Therefore taking other lower levels to estimate M should bias the results by giving too much weight to the lower sources, resulting in lower values for M. Note, however, that if we take the four upper levels (between 14 and 38 m) we get values for M and P that are only 2 and 5% smaller than the values obtained with the 25-m level but with a smaller standard deviation (Table 2).

[49] From equation (13) (see also Appendix B) we can see that M is the ratio of the eddy isoflux to the eddy flux and is likely to change during the day. In Figure 7 we plotted these two eddy fluxes and their ratio, either predicted by MuSICA or estimated from measurements. The results have been bin averaged over the whole 22-day period. The eddy isoflux computed with equation (13) (solid circles) is in excellent agreement with MuSICA (solid line), especially in the afternoon (Figure 7a). This is also the case for the measured and modeled eddy CO_2 flux (Figure 7b, see also Figure 3). It is therefore not surprising to see that the ratio of the two eddy fluxes given by MuSICA is rather stable in the afternoon and close to the value of −23.6‰ derived from the C_a and δ_a measurements at 25 m (Figure 7c). On the other hand, before noon and in the evening the model predicts rapid and large fluctuations of M with a strong day-to-day variability. The eddy isoflux can be seen as the difference of the isoflux and the isostorage. Both terms are likely to vary strongly in the morning and the evening as they depend on $\delta_a - \Delta_a$ and turbulence, respectively. Therefore the variations of M predicted by MuSICA in the morning and the evening are likely to be real. Nonetheless, the amplitude given by MuSICA is probably amplified by numerical instability as we saw earlier that MuSICA encounters difficulties to converge when the sensible heat flux is dominated by the air storage term.

[50] In the light of Figure 7c we could think that the estimation of M and the $C_a\delta_a$ versus C_a linear regression could be made with C_a and δ_a measurements performed in the afternoon only. In fact such a regression is inaccurate because C_a and δ_a variations are too small in the afternoon (not shown, but see Figure 8b below). Indeed, when only afternoon C_a and δ_a measurements are considered the resulting M value lies very far (less than −40‰) from the values given by MuSICA or the value of −23.6‰ obtained

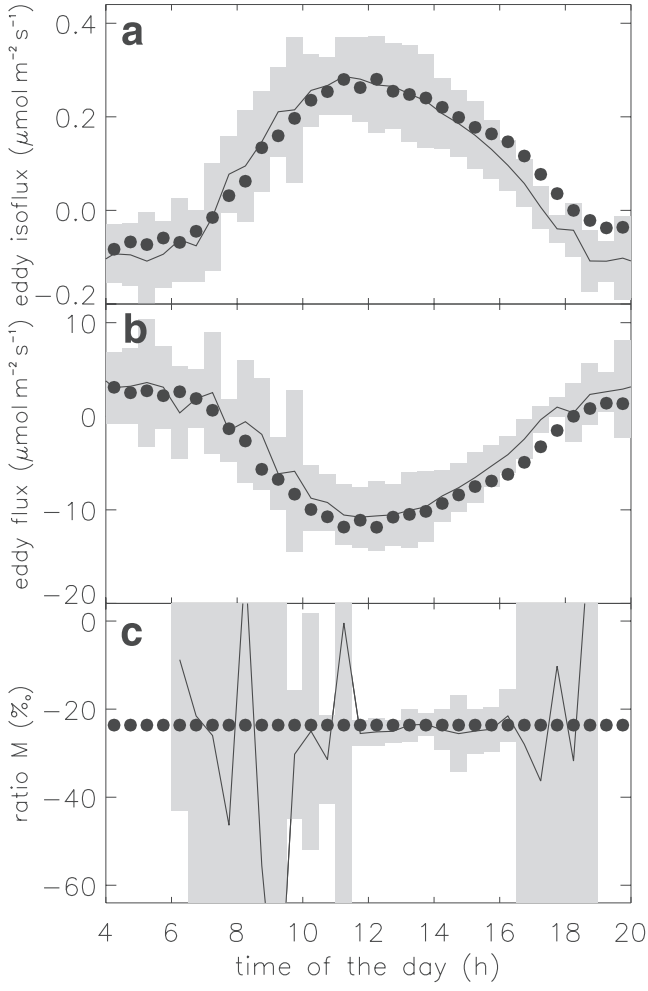

Figure 7. Bin-averaged measured (solid circles) and modeled (solid line) (a) eddy isoflux, (b) eddy flux, and (c) their ratio M = eddy isoflux/eddy flux. For modeled values we indicated in gray the standard deviation resulting from bin averaging over the 22-day period (4–25 September 1997). In Figure 7c, the measured value corresponds to M = −23.6‰ (equation (13)) and was estimated from CO_2 and $^{13}CO_2$ measurements at 25 m (Table 2).

with all time steps. Even if it seems theoretically not fully satisfying, the morning values are crucial to determine M accurately. Increasing the accuracy of C_a and δ_a profiles in the afternoon may also overcome the problem.

4.5. Determination of the Isostorage

[51] CO_2 storage is needed to compute NEE (right-hand side of equation (4a)). Similarly, the isostorage is needed to compute the isoflux (right-hand side of equation (4b)). The values of δ_a at all levels over the whole period are then necessary.

[52] CO_2 measurements were available at all levels and over the 22-day period but $^{13}CO_2$ measurements were only available over a 24-hour period. We then performed level-by-level linear regressions between daytime $C_a\delta_a$ and C_a data. The slope of these regressions corresponds to the values plotted in Figure 6 and the regression at 25 m already gave us M and P.

[53] We used these regression outputs, the nighttime regression results (used to determine δ_r) and the CO_2 measurements to construct continuous variations of $^{13}CO_2$ at all levels and over the whole 22-day period. This allowed us to compute the "measured" isostorage. The resulting δ_a values at 25 m were also used to run the MuSICA model over the whole period.

[54] Figure 8 shows the measured and modeled values of the isostorage and the resulting isoflux. The results have been bin averaged over the 22-day period. We can see that the agreement between model and measurements are good during the day except around 0800–1000 hours when the measurements seem to indicate a greater flush out of $^{13}CO_2$ than the model. The same tendency is observed between measured and modeled CO_2 storage and NEE (not shown). The fact that MuSICA has difficulties to capture the scalar profiles (and consequently, the storage terms) in the early morning may explain the disagreement. However, the measured NEE is computed as the sum of the measured eddy flux and the measured CO_2 storage but the modeled NEE is independent of the modeled CO_2 storage. It is therefore surprising to see that the model is unable to capture the NEE variations at this time of the day while it behaves well at other periods. This may indicate that the measurements (concerning the air storage or the eddy flux) are themselves erroneous at this time of the day. Overall it is difficult to know which isostorage, between the model and the measurements, is the most realistic.

4.6. Determination of the Canopy Conductance

[55] We evaluated the ability of the Penmann-Monteith equation to retrieve a canopy conductance g_c. For this we applied equation (9) over the 22-day period using the energy and radiative flux measurements available at our site. The results are bin averaged over the whole period and are shown in Figure 9a. We also plotted the bulk canopy conductance predicted by the MuSICA model with its standard deviation over the period. The computation of this bulk canopy conductance from the modeled stomatal conductances of each leaf is not unique and two different definitions may result in large discrepancies [*Finnigan and Raupach*, 1987]. We chose the definition of Finnigan and Raupach because it is directly derived from the Penmann-Monteith equation which ensures conservation of the total latent heat flux (see Appendix C).

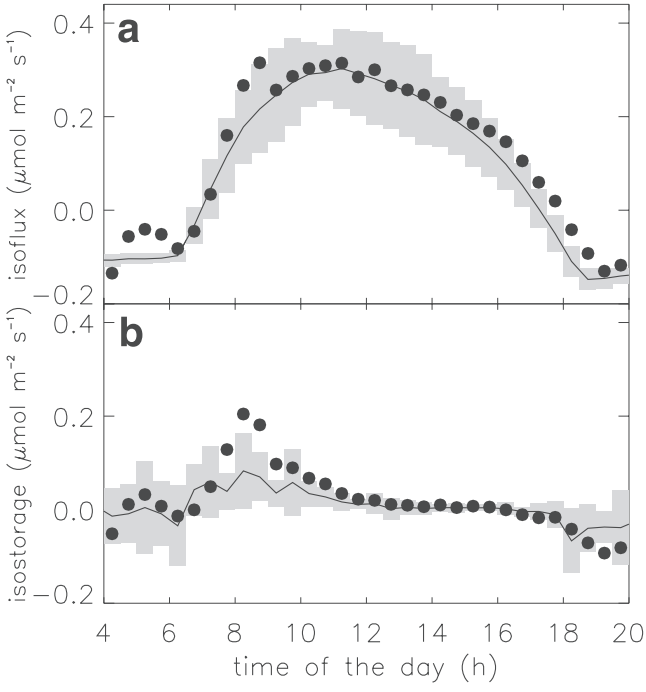

Figure 8. Bin-averaged measured (solid circles) and modeled (solid line) (a) isostorage and (b) isoflux = eddy isoflux + isostorage. For modeled values we indicated in gray the standard deviation resulting from bin averaging over the 22-day period (4–25 September 1997).

[56] Figure 9a shows that the diurnal pattern is similar for both canopy conductances. However, we notice that the Penmann-Monteith equation gives bin-averaged g_c values slightly smaller than the bulk canopy conductance given by the MuSICA model. It has to be pointed out that LE encloses not only transpiration from the vegetation but also soil evaporation, which should rather enhance the bulk canopy conductance from the Penmann-Monteith equation. Larger g_c values of MuSICA compared to the Penmann-Monteith equation may be explained by discrepancies in the energy budget closure observed over the 22-day period. Indeed, the sum of the turbulent fluxes H and LE only represents 84% of the available energy $R_n - G$ (not shown) which causes an underestimation of the bulk canopy conductance estimated with the Penmann-Monteith equation (see equation (9)).

[57] Figure 9b shows the aerodynamic conductance g_a computed according to equations (10) and (11). This conductance is 3–4 times smaller than the area-weighted average of the leaf boundary layer conductances (not shown, see Appendix C) but is still an order of magnitude greater than g_c. The aerodynamic conductance g_a therefore has a relatively small impact on the computation of Δ_A and on the retrieval of F_A and F_R.

[58] Figure 9c shows the bulk mesophyll conductance $g_m = 1/r_m$ given by the MuSICA model. This bulk conductance is computed from leaf conductances at the

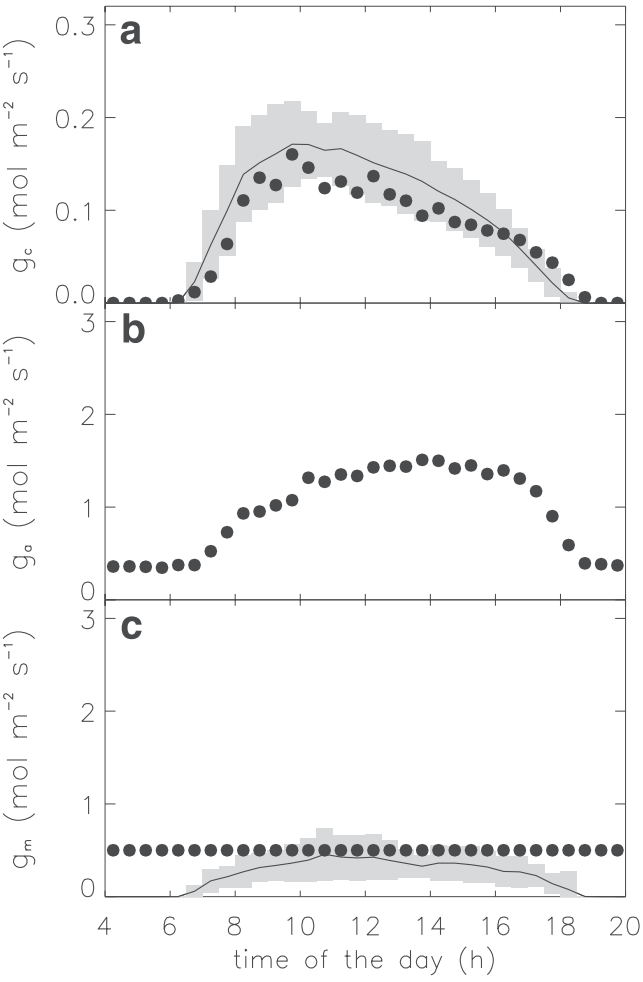

Figure 9. Bin averaged from Penmann-Monteith (solid circles) and modeled (solid line) conductances: (a) bulk canopy conductance, (b) aerodynamic conductance, and (c) bulk mesophyll conductance. For modeled values we indicated in gray the standard deviation resulting from bin averaging over the 22-day period (4–25 September 1997).

leaf level in a way similar to the computation of g_c (see Appendix C). In MuSICA the mesophyll conductance is set at 0.5 mol m^{-2} s^{-1} for understorey leaves and 0.125 mol m^{-2} s^{-1} for canopy needles [*Loreto et al.*, 1992]. The resulting bulk mesophyll conductance varies from 0 to 0.5 mol m^{-2} s^{-1} (Figure 9c) because it has been weighted with leaf assimilation. We took the maximum value (0.5 mol m^{-2} s^{-1}) in equations (7) and (8) to estimate F_A and F_R because it corresponds to the average midday value. Note that *Bowling et al.* [2001] neglected the mesophyll resistance $1/g_m$ compared with the bulk canopy resistance $1/g_c$. In their case the expression for $\overline{a}$ reduces to $\overline{a} = a = 4.4‰$ and equation (8) becomes $-F_A = g_c(C_a - C_c)$. Such a simplification is not possible in our case because g_m is only 2–3 times as large as g_c.

4.7. Retrieval of F_R, F_A, and Δ_a

[59] First, we found it important to illustrate the difference between F_R and TER (or F_A and GPP). The values of F_R and F_A (solid line) and TER and GPP (dashed line) obtained with MuSICA over the 22-day period are shown in Figures 10a and 10b. As for the preceding variables the results have been bin averaged. TER estimates can also be obtained from a regression of nocturnal NEE versus soil temperature, but for our study, such a regression was inaccurate because of the small range of soil temperature during the 22-day period. However, using the regression of *Berbigier et al.* [2001] (obtained at the same site after 2 years of eddy-flux measurements) would give almost the same TER and GPP curves (not shown). We can see in Figure 10a that F_R is 30–50% smaller than TER during the day, with little day-to-day variability. The difference between F_A and GPP is proportionally much smaller and within the range of the

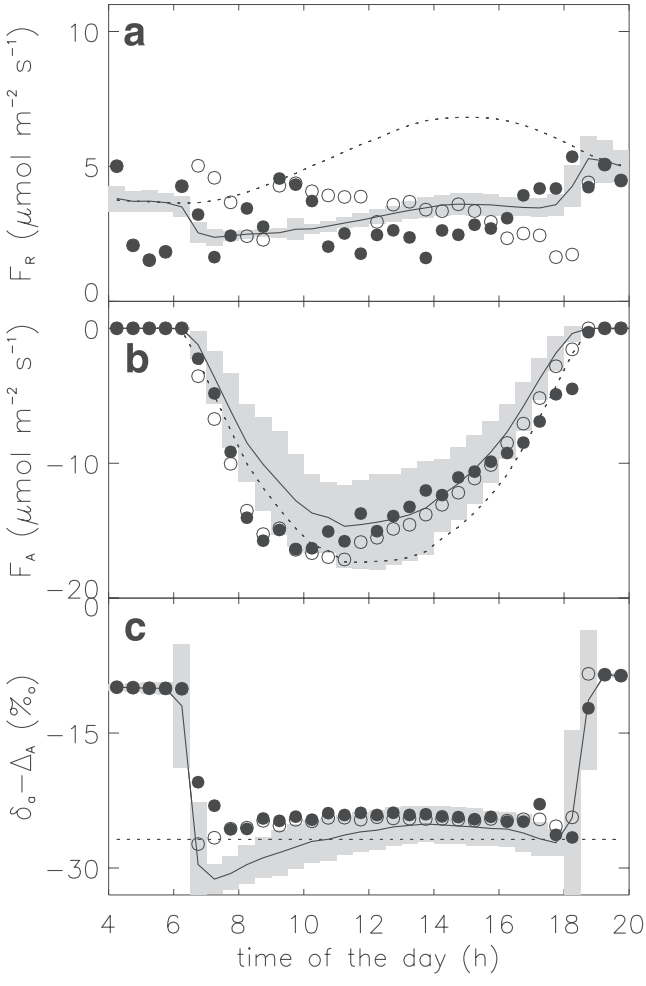

Figure 10. Bin-averaged measured (circles) and modeled (solid line) (a) nonfoliar respiration, (b) net assimilation, and (c) ecosystem fractionation toward $^{13}CO_2$. For measured values we plotted values computed with g_c given either by the Penmann-Monteith equation (solid circles) or by the MuSICA model (open circles). In this latter case g_m was also given by MuSICA. For modeled values we indicated in gray the standard deviation resulting from bin averaging over the 22-day period (4–25 September 1997). The dotted curve represents bin-averaged modeled TER and GPP (Figures 10a and 10b, respectively) or δ_r (Figure 10c).

day-to-day variability in F_A. This is because TER mainly depends on soil temperature and moisture which vary slowly during the period of study, while GPP depends on several environmental factors such as radiation, air VPD or wind speed, and is likely to vary strongly from one day to the next. It is clear from Figure 10a that it is not possible to validate the method of Bowling et al. (that separates NEE into F_R and F_A) by comparing the results to TER and GPP estimates. A model such as MuSICA, which gives independent F_A and F_R estimates, is necessary to validate this method.

[60] The fractionation factor Δ_A is a linear function of F_A (see equations (6) and (8)) so that equation (4b) can be rewritten as a quadratic equation in F_A [*Bowling et al.*, 2001]. This equation is solved for F_A according to *Press et al.* [1992] and F_R is given by equation (4a). The resulting F_R and F_A values for the 22-day period have been bin averaged and plotted in Figures 10a and 10b (solid circles). The agreement with the F_R and F_A values predicted by MuSICA is rather good, especially in the afternoon where it remains within 15–20% at most time steps. In the morning (around 0800–1000 hours) F_R values given by equation (4a) are overestimated compared to those given by MuSICA and become closer to TER. However, this disagreement lies within the day-to-day variability of F_A (Figure 10b). The reason for this disagreement is explained below.

[61] As mentioned by *Bowling et al.* [2001] the EC/flask method is very sensitive to g_c. Indeed, when we take g_c given by MuSICA rather than the Penmann-Monteith equation this gives quite different F_R and F_A values (not shown). A better agreement is obtained when we use simultaneously g_c and g_m given by MuSICA. The resulting F_R values (open circles in Figures 10a and 10b) are then close to those given by MuSICA, especially in the midafternoon (1200–1700 hours) where the agreement approaches 5–10%, but remains overestimated and closer to TER in the morning.

[62] In fact the quadratic equation of F_A may sometimes have no real solution. In this case F_R is not computed and not accounted for in the bin averaging. Such a situation occurs when $\delta_a - \Delta_A$ is close to δ_r. We plotted in Figure 10c the bin-averaged $\delta_a - \Delta_A$ values given by MuSICA and by equations (6) and (8). The model predicts that isotopic equilibrium (i.e., $\delta_a - \Delta_A = \delta_r$) is more often satisfied in the morning (around 0900–1100 hours) and before sunset (around 1800 hours). The bin-averaged $\delta_a - \Delta_A$ values given by equations (6) and (8) are therefore not representative of the whole period and should not be trusted at this time of the day. In other words, the EC/flask method works better at certain times of the day than others. The period at which it works best is in the midafternoon (around 1400–1600 hours), when Δ_A takes its minimum absolute value and the isotopic disequilibrium is strong. Fortunately, F_R has a small amplitude during daytime so that the value at 1400–1600 hours is representative of the whole day.

[63] This result and other results from the preceding sections help us formulate an efficient and cost-effective sampling strategy.

4.8. Retrieval of F_R and F_A From a Data Subset

[64] Our objective here is to consider the possibility to retrieve F_R and F_A on a routine basis with the EC/flask method of *Bowling et al.* [2001]. We saw that with the full data set of isotopic measurements (341 flasks over a 24-hour period) we were able to retrieve correctly F_R and F_A over a longer period (within 15–20%). However, this experimental setup is obviously too heavy to be implemented on a routine basis. The next step is to determine a subset of isotopic data that would allow us to retrieve F_R and F_A (or rather their mean daytime value) with a similar accuracy.

[65] Nighttime isotopic measurements are needed to estimate δ_r. We saw that the estimation of δ_r depends on sampling: the overall nighttime data set gives a value of −26.8‰ but the same data set gives different values when it is subsampled by levels (−26.3‰ at 25 m) or by time steps (−27.1‰ on an average). However, the scatter between δ_r values at different time steps remains within the range of measurement errors (0.3‰). We can therefore imagine to use only C_a and δ_a measurements at one or two time steps only but from several levels. It seems preferable to reduce the number of levels within the vegetation in order to reduce the possible impact of foliar respiration on the determination of δ_r. If we only take one isotopic measurement by vegetation layer, i.e., at 25 m, within the canopy, below the canopy, in the understorey, and at the ground, we then have to analyze only 5 or 10 flasks instead of the 187 flasks collected at night during our 24-hour campaign.

[66] Daytime isotopic measurements are used to estimate M and the corresponding eddy-isoflux ,and to compute the isostorage during the day. The estimation of M is made with the isotopic measurements at 25 m only. Several time steps are therefore needed to get an accurate value, but four or five isotopic measurements are sufficient. We saw in the preceding section that F_R had a small amplitude during daytime. We can therefore estimate F_R at times of the day when the EC/flask method works best (in midafternoon, when the ecosystem is far from isotopic equilibrium) and extrapolate the results to the whole daytime period. We pointed out that M could not be determined from afternoon values only because the range of variation in C_a and δ_a is too small at this period of the day. Such a behavior is general and has been observed at a variety of sites [e.g., *Buchmann et al.*, 1997]. Our subset of isotopic data should therefore contain $^{13}CO_2$ measurements in the morning (to determine M) and in the afternoon (when the EC/flask method works best).

[67] In theory, isostorage requires $^{13}CO_2$ measurements at all levels in order to perform linear regressions between $C_a\delta_a$ and C_a, and to get continuous δ_a values at all levels. As can be seen in Figure 6, the regression differs from one level to the next. As a sensitivity test, we computed the isostorage from δ_a values estimated with the regression found at 25 m only. The resulting isostorage is not significantly different from the isostorage plotted in Figure 8b (not shown) and leads to almost the same F_R/F_A estimates. Therefore the isotopic measurements at levels other than 25 m do not seem crucial during daytime. The four or five isotopic measurements during the day should therefore be sufficient to estimate both M and the isostorage. By comparison, for our 24-hour campaign, we collected 14 flasks at 25 m during daytime and the same amount of flasks was collected at the other 10 levels.

Table 3. Mean Nonfoliar Respiration Over the 22-Day Period Predicted by Different Approaches (PM = Penmann-Monteith Equation) and Sampling Strategies[a]

	$\langle F_R \rangle$, g C m^{-2} d^{-1}
MuSICA model	3.8 (3.7)
Full data set	
g_c (PM) with g_m = 0.5 mmol m^{-2} s^{-1}	3.3 (3.1)
g_c (MuSICA) with g_m(MuSICA)	3.4 (3.5)
Subset of data	
g_c (PM) with g_m = 0.5 mmol m^{-2} s^{-1}	3.2 (3.2)
g_c (MuSICA) with g_m(MuSICA)	3.4 (3.4)
g_c (PM) without g_m	5.3 (4.8)
g_c (MuSICA) without g_m	6.8 (6.8)

[a]In parentheses we give the results when the mean is computed with only four values during the day (0700, 0800, 1400, and 1500 hours), assuming that F_R does not change much during the day.

[68] We subsampled our data set by taking only two nighttime $^{13}CO_2$ profiles (at 2400 and 0100 hours) with only five levels (25, 14, 6, 0.7, and 0.01 m) and four daytime $^{13}CO_2$ values (0700, 0800, 1400, and 1500 hours). We then obtained $\delta_r = -27.3 \pm 0.6‰$ and $M = -23.7 \pm 1.0‰$, compared to $-26.8 \pm 0.1‰$ and $-23.6 \pm 0.7‰$ with the full data set, respectively. The isostorage was also not significantly different than that computed with the full data set.

[69] We then partitioned NEE into F_R and F_A. Results are presented in Table 3 in terms of mean daytime nonfoliar respiration $\langle F_R \rangle$. We can see that values obtained with our subset of data are not very different from those obtained with the full data set. In all cases they are about 15–20% smaller than the value given by MuSICA, which must be considered as the order of magnitude of the accuracy of the EC/flask method.

[70] Finally, we tested the effect of neglecting the mesophyll resistance $1/g_m$ compared with the bulk canopy resistance $1/g_c$ on the retrieval of F_A and F_R. Indeed, the estimation of a bulk mesophyll conductance for a given ecosystem is not easy and very few data are available in the literature. Table 3 shows that the $\langle F_R \rangle$ value is in this case much greater than before (around 6 g C m^{-2} s^{-1} depending on the choice of g_c) and than the average TER given by MuSICA (5.1 g C m^{-2} s^{-1}). This is because the total conductance in equation (8) and thus F_A are then overestimated. Such a simplification is therefore impossible in our case and we need to prescribe a value for g_m to perform the partitioning. The results may be different at other sites with a greater mesophyll conductance. Nevertheless, before applying the EC/flask method to partition F_R and F_A at a given site one must have an idea of the value of the mesophyll conductance, as compared with the stomatal conductance.

5. Conclusions

[71] In this paper we investigated the possibility to estimate F_R and F_A at one FluxNet site from continuous CO_2 flux and concentration measurements and intensive $^{13}CO_2$ measurements. For this we applied the EC/flask method of *Bowling et al.* [2001] and used the multilayer model MuSICA as a perfect simulator to test each underlying hypothesis and evaluate the partitioning. The idea was to apply this method on a routine basis, i.e., by collecting less isotopic measurements at each campaign, but more regularly during one growing season. Our objective was then to formulate an efficient and cost-effective strategy to get the best subset of isotopic measurements to perform the partitioning of NEE into F_R and F_A. The method can be decomposed into different steps (Figure 1).

[72] First, we needed to estimate the daytime isotopic signature δ_r of nonfoliar respiration. For this we made a $C_a\delta_a$ versus C_a linear regression using measurements collected during one night at different levels above and within the vegetation, and identified δ_r as the slope of this regression. The value of δ_r estimated with the full data set was $-26.8 \pm 0.1‰$, in close agreement with the isotopic content of soil organic matter and plant biomass (Table 1b). Such determination of δ_r relies on the assumptions that δ_r is constant with time and that foliar and nonfoliar or nighttime and daytime respiration rates have the same isotopic signature. Making a regression for each time step or at each level revealed that the value of δ_r changed little during the night (Table 1a), but the slope of the regression appeared to differ significantly from one level to the next (Figure 5a), with higher values in the vegetative layers. Such a situation would occur if foliar respiration was enriched compared to nonfoliar respiration. In this case it would be problematic to estimate δ_r with our method as one of the underlying assumptions would not hold. Other campaigns are therefore needed to confirm this result. To go one step further we also ran MuSICA with a range of isotopic signatures for the CO_2 respired by leaf elements. In all simulations the model predicted C_a and δ_a values that never lead to such vertical variations of δ_r, as those obtained with the experimental data. One possible explanation is that the turbulent transfer module used in MuSICA overestimates the air mixing in the vegetative layers as has already been observed in a previous study [*Warland and Thurtell*, 2000]. Other turbulent transfer theories need to be tested to explore this possibility. We conclude that despite the dense vertical and temporal resolution of this experimental study and the refinement of the MuSICA model, it was not possible to confirm that the assumptions underlying the determination of δ_r were verified at our site. Assuming that they are, a cost-effective sampling strategy to estimate δ_r is to measure one or two $^{13}CO_2$ profiles during the night with four or five levels only, preferentially not in the vegetative layers.

[73] Secondly, we had to estimate the eddy isoflux. For this we showed that the use of equation (13) was more accurate than its first-order approximation (equation (5)) because it is $C_a\delta_a$ and not δ_a alone that is linearly related to C_a (see Appendix B). We then made a $C_a\delta_a$ versus C_a linear regression using daytime measurements at 25 m to estimate the slope M to be used in equation (13). We used the measurements at 25 m only because it is the level at which the eddy flux was performed. We showed that using other levels (not too close to the canopy top) would not lead to very different values of M (Figure 6 and Table 2). We also showed that the estimation of M could not be performed without a certain range of variations of C_a and δ_a and that the early morning values are crucial to get an accurate value for M. For this reason we conclude that the best strategy to estimate M is to perform $^{13}CO_2$ measurements at one level

(where the eddy flux is measured) and in the early morning (around 0700–0800 hours solar time) and in the afternoon (around 1400–1600 hours).

[74] Thirdly, we needed to estimate the isostorage. For this we used the CO_2 profiles and the regressions used to determine δ_r and M to construct a continuous data set of $^{13}CO_2$ values. The use of a regression level by level during the day (which was possible because $^{13}CO_2$ measurements were performed at the same 11 levels than CO_2 measurements) changed only slightly our estimates of the isostorage, especially in the midafternoon. The regressions giving δ_r and M are therefore sufficient to retrieve a continuous data set of $^{13}CO_2$ values and estimate the isostorage, as long as we perform continuous CO_2 measurements at different levels.

[75] Fourth, we had to estimate the bulk canopy and mesophyll conductances. The Penmann-Monteith equation is quite robust to estimate g_c and we verified it with our data set. The bulk mesophyll conductance is difficult to estimate but appears to play an important role in the partitioning exercise. It is therefore crucial to get an estimate of the relative importance of the mesophyll conductance compared with the stomatal conductance if we want to get accurate estimates of F_R and F_A.

[76] With our full data set we were able to retrieve F_A and F_R values in agreement with the MuSICA model within 15–20%. We showed that the EC/flask method works better in midafternoon when Δ_A takes its minimum absolute value and isotopic disequilibrium is strong. Using the subset of data allowed us to retrieve average F_A and F_R values that agree with MuSICA within 15–20% also. This was made possible because F_R does not have a marked diurnal cycle.

[77] This study allowed us to define the best cost-effective sampling strategy to estimate F_R and F_A from continuous CO_2 flux and concentration measurements, and intensive $^{13}CO_2$ measurements. In the future we need to check whether the conditions of occurrence of isotopic disequilibrium vary or not with species or throughout the growing season. It is clear that the minimum of Δ_A should always occur in midafternoon when we have the highest levels of vapor pressure deficit. Indeed, this strong evaporative demand forces the stomata to close but little affects the rate of photosynthesis so that the ratio C_c/C_a and Δ_A are lower. However, the daily minimum of Δ_A, and the values of δ_a and δ_r should vary throughout the season, and some days isotopic disequilibrium may never occur. Additional studies at other seasons and other sites are now needed to check whether the retrieval of F_A and F_R can really be performed throughout the season within a 15–20% confidence interval.

Appendix A

A1. MuSICA and the Transport of $^{13}CO_2$

[78] The multilayer multileaf soil-vegetation-atmosphere transfer model MuSICA is extensively described elsewhere [*Ogée et al.*, 2003]. Equations for the transport of $^{13}CO_2$ have been added for the present study and are presented here.

A1.1. Turbulent Transfer in MuSICA

[79] The total air concentration of a given scalar (for example $C_{a,k}$ for CO_2) at any level z_k is computed with a Lagrangian turbulent transfer scheme summarized in the equation [*Baldocchi and Harley*, 1995; *Raupach*, 1989a]:

$$C_{a,k} - C_{a,r} = \sum_{j=1,n} D_{kj} S_j \Delta z_j + D_{k0} F_0, \qquad \text{(A1)}$$

where $C_{a,r}$ (μmol m^{-3}) is the total CO_2 concentration at a reference level z_r above vegetation, S_j (μmol m^{-3} s^{-1}) is the total CO_2 source/sink density of vegetation layer j with thickness Δz_j (m), n is the number of vegetation layers, and D_{kj} (s m^{-1}) is the turbulent dispersion matrix. The latter depends solely on turbulence statistics and is computed according to the localized near-field theory [*Raupach*, 1989b]. F_0 (μmol m^{-2} s^{-1}) is the total CO_2 efflux that emanates from the forest floor.

[80] In each canopy layer we distinguish 12 types of big leaves (or big shoots) according to their age (1-, 2-, or 3-year-old), sun exposure (sunlit or shaded), and water status (wet or dry). In the understorey layer we distinguish only four big leaves because they belong to a single age class. The CO_2 source/sink density of vegetation layer j with thickness Δz_j can be expressed as:

$$S_j = - \sum_{\substack{\text{type}=1,p \\ \text{dry}}} \ell_{\text{type},j} A_{n,\text{type},j} \Delta z_j + F_{\text{bole},j}, \qquad \text{(A2)}$$

where $\ell_{\text{type},j}$ (m^2 m^{-3})is the leaf area density of the big leaf of type "type" in layer j, $A_{n,\text{type},j}$ (μmol m^2 s^{-1}) is its net CO_2 exchange rate with surrounding air, and $F_{\text{bole},j}$ (μmol m^2 s^{-1}) is the bole respiration rate. The summation in equation (A2) is restricted to dry big leaves only because wet leaves are not supposed to exchange CO_2 with the atmosphere.

[81] $C_{a,k}$ can be decomposed into various isotopic concentrations. For each of these an equation similar to equation (A1) applies. For example, for $^{13}CO_2$:

$$C^{13}_{a,k} - C^{13}_{a,r} = \sum_{j=1,n} D_{kj} S^{13}_j \Delta z_j + D_{k0} F^{13}_0, \qquad \text{(A3)}$$

where superscript "13" denotes the same quantities as for the total scalar concentration but for the $^{13}CO_2$ isotopic concentration only. In δ notation we have:

$$C_{a,k}\delta_{a,k} - C_{a,r}\delta_{a,r} = \sum_{j=1,n} D_{kj} S_j \Delta z_j \delta_j + D_{k0} F_0 \delta_0, \qquad \text{(A4)}$$

where δ_j represents the isotopic composition of source S_j and is defined by $(1 + \delta_j)\, R_{\text{PDB}} = S^{13}_j / S_j$ and $(1 + \delta_0)\, R_{\text{PDB}} = F^{13}_0 / F_0$ where R_{PDB} is the isotopic composition of the Pee Dee Belemnite standard. It usually depends linearly on the air isotopic composition of the air (see below) so that we can write:

$$\delta_j = a_j \delta_{a,j} + b_j \quad \text{and} \quad \delta_0 = a_0 \delta_{a,1} + b_0. \qquad \text{(A5)}$$

[82] Equation (A4) can therefore be rewritten as

$$\sum_{j=1,n} A_{kj}\delta_{a,j} = B_k \qquad (k = 1, n). \tag{A6}$$

[83] This equation can be solved in deltas. The expressions of the coefficients A_{kj} and B_k are related to coefficients a_j and b_j by:

$$\begin{cases} A_{kj} = \varepsilon_{kj}C_{a,k} - D_{kj}\Delta z_j a_j - \varepsilon_{k1}D_{k0}a_0 \\ B_k = C_{a,r}\delta_{a,r} + \sum_{j=1,n} D_{kj}\Delta z_j b_j + D_{k0}b_0, \end{cases} \tag{A7}$$

where ε_{kj} equals 1 if $k = j$, and 0 otherwise.

A1.2. Expression of the Coefficients a_j and b_j for $^{13}CO_2$

[84] The CO_2 source/sink density of vegetation layer j is given by equation (A2). For $^{13}CO_2$ we have:

$$S_j^{13} = -\sum_{\substack{\text{type}=1,\,p \\ \text{dry}}} \ell_{\text{type},j} A_{n,\text{type},j}^{13}\Delta z_j + F_{\text{bole},j}^{13}. \tag{A8}$$

[85] The same notations as in equation (A2) are used but with superscript 13 for $^{13}CO_2$ assimilation and bole respiration rates.

[86] The $^{13}CO_2$ assimilation rate of a dry assimilating ($g_s > 0$) leaf is computed according to *Farquhar et al.* [1989] and the $^{13}CO_2$ exchange rate of a dry nonassimilating ($g_s = 0$) leaf is simply expressed as the product of the respiration rate and the $^{13}CO_2/CO_2$ isotopic composition of "freshly respired sugars" ($\delta_{\text{type},j}$). The $^{13}CO_2$ bole respiration rate in layer j is also expressed as the product of the bole respiration rate ($F_{\text{bole},j}$) and the $^{13}CO_2/CO_2$ isotopic composition of freshly respired sugars ($\delta_{\text{bole},j}$). We then get:

$$\begin{cases} a_j = \sum_{\substack{\text{type}=1,\text{p} \\ \text{dry},g_s>0}} \ell_{\text{type},j} A_{n,\text{type},j} \\ b_j = \sum_{\substack{\text{type}=1,\text{p} \\ \text{dry},g_s>0}} \ell_{\text{type},j} A_{n,\text{type},j}\Delta_{A,\text{type},j} \\ \qquad + \sum_{\substack{\text{type}=1,\text{p} \\ \text{dry},g_s=0}} \ell_{\text{type},j} A_{n,\text{type},j}\delta_{\text{type},j} + F_{\text{bole},j}\delta_{\text{bole},j}, \end{cases} \tag{A9}$$

where $\Delta_{A,\text{type},j}$ is given by equations similar to equations (6) and (7). If we decompose the soil CO_2 efflux into microbial and root respiration ($F_0 = F_{\text{microb}} + F_{\text{root}}$) with two different isotopic compositions (δ_{microb} and δ_{root}) we get:

$$\begin{cases} a_0 = 0 \\ b_0 = F_{\text{microb}}\delta_{\text{microb}} + F_{\text{root}}\delta_{\text{root}}. \end{cases} \tag{A10}$$

[87] In the present version of MuSICA the isotopic compositions $\delta_{\text{bole},j}$, $\delta_{\text{type},j}$, δ_{root}, and δ_{microb} are prescribed, and not allowed to change over time.

A1.3. Parameterization of MuSICA

[88] The parameterization of MuSICA is that used by *Ogée et al.* [2003] at the same site, except that soil respiration at 15°C has been reduced by 50%. This modification was necessary to account for the effect of low soil water levels on soil respiration [*Ogée et al.*, 2003]. In addition, leaf mesophyll conductances have been included in the model because the discrimination factors $\Delta_{A,\text{type},j}$ depend on chloroplastic, not internal, CO_2 concentration. During the computation of leaf assimilation ($A_{n,\text{type},j}$) these conductances are set to an infinite value for keeping the model consistent with the set of values used for the parameterization of the photosynthesis model, all established on an internal, not chloroplastic, CO_2 basis. The model then relates the chloroplastic CO_2 concentration to $A_{n,\text{type},j}$ and the internal CO_2 concentration.

Appendix B: Relationship Between $C\delta$ and C

[89] The surface boundary layer above vegetation is divided into two regions: the inertial sublayer above a level conventionally referred to as z_* (on the order of 2 to a few times the vegetation height h) and the roughness sublayer below this level.

[90] Using similarity theory principles *Cellier and Brunet* [1992] found that, for any atmospheric tracer X, the vertical gradient above vegetation ($h < z < z_*$) can be expressed as:

$$\frac{dX}{dz} = \frac{X_*}{kz_*}\phi_x(\zeta) \quad \text{with} \quad X_* = -\frac{\overline{w'X'}}{U_*}, \tag{B1}$$

where X_* is the scalar turbulent flux normalized by U_*, ϕ_x and ζ are a nondimensional stability function and a stability parameter, respectively, and k is the von Karman constant (0.4).

[91] The stability parameter ζ is usually taken equal to h/L in the roughness sublayer, where L is the Obukhov length scale [*Jacobs et al.*, 1992; *Leclerc and Beissner*, 1990; *Shaw et al.*, 1988]. In this case the gradient dX/dz is constant between h and z_*. For two scalars, here C_a and $C_a\delta_a$, this means that their gradients are proportional in this region:

$$\begin{cases} dC_a = m_1\, dz \\ d(C_a\delta_a) = m_2\, dz \end{cases}. \tag{B2}$$

[92] We should therefore express $C_a\delta_a$ in terms of C_a to compute the eddy isoflux. Note that the linear relationship between $C_a\delta_a$ and C_a should not depend on atmospheric stability (assuming that the stability function is the same for both scalars) but only on the ratio of the two scalar turbulent fluxes. If we neglect storage terms in equation (4) (which is possible in midafternoon for instance), the coefficient M is then equal to $\delta_r + (\delta_a - \Delta_A - \delta_r)F_A/(F_A + F_R)$.

[93] Writing $d(\delta_a C_a) = \delta_a dC_a + C_a d\delta_a$ we also get:

$$d\delta_a = \frac{m_2 - m_1}{m_1 C_a} dC_a. \tag{B3}$$

[94] Over the range of variation in atmospheric CO_2 concentration, $1/C_a$ can be considered as nearly constant. At this first-order approximation we then have proportionality between C_a and δ_a gradients, as was empirically assumed by *Bowling et al.* [2001], and we can also express δ_a in terms of C_a to compute the eddy isoflux.

[95] These linear relationships should actually vary from one time step to the next and a different value for M should be used to compute the eddy isoflux at each time step. Yet a single linear relationship seems to hold during the full daytime period (Table 2; see also *Bowling et al.* [2001]). This is partly explained by the fact that $\delta_a - \Delta_A$ is close to δ_r and steady for most of the day (Figure 10c).

Appendix C: Bulk Canopy and Mesophyll Conductances

[96] The Penmann-Monteith equation at the canopy scale is:

$$\mathrm{LE} = \frac{(s/0.92\gamma)(R_n - G) + \rho L g'_a D_a}{s/0.92\gamma + 1 + g'_a/g'_c}. \tag{C1}$$

[97] The primes denote conductances for water vapor instead of CO_2. This equation can also be applied at each big leaf within the canopy:

$$\mathrm{LE} = \sum_{j=1,n} \sum_{\substack{\mathrm{type}=1,p \\ \mathrm{dry}}} \ell_{\mathrm{type},j} \left[\frac{(s/0.92\gamma) Q_{\mathrm{abs,type},j} + \rho L g'_{b,\mathrm{type},j} D_{a,j}}{s/0.92\gamma + 1 + g'_{b,\mathrm{type},j}/g'_{s,\mathrm{type},j}} \right] \Delta z_j, \tag{C2}$$

where $g_{b,\mathrm{type},j}$ and $g_{s,\mathrm{type},j}$ are the boundary layer and the stomatal conductances of big leaf of type "type" in layer j, respectively. If we assume that turbulence is well mixed then $D_{a,j}$ in equation (C2) can be replaced by D_a. Then in the limit of potential evaporation ($g_c \to \infty$, $g_{s,\mathrm{type},j} \to \infty$), identification of the terms in D_a and $R_n - G$ in equations (C1) and (C2) leads to [*Finnigan and Raupach*, 1987]:

$$\begin{cases} g'_a = \sum_{j=1,n} \sum_{\substack{\mathrm{type}=1,p \\ \mathrm{dry}}} \ell_{\mathrm{type},j}\, g'_{b,\mathrm{type},j}\, \Delta z_j \\ R_n - G = \sum_{j=1,n} \sum_{\substack{\mathrm{type}=1,p \\ \mathrm{dry}}} \ell_{\mathrm{type},j}\, Q_{\mathrm{abs,type},j}\, \Delta z_j \end{cases}. \tag{C3}$$

[98] Hence g_a and $R_n - G$ are simply the sum of their area-weighted counterparts at the leaf scale. We then computed g_c from equation (C1) (see equation (9)), and substituting for $R_n - G$, g_a, and LE in terms of leaf variables, from equations (C2) and (C3).

[99] The bulk mesophyll conductance is computed in the same framework. Net assimilation F_A is given by equation (8) in terms of bulk conductances. In MuSICA this flux is computed according to:

$$-F_A = \sum_{j=1,n} \sum_{\substack{\mathrm{type}=1,p \\ \mathrm{dry},g_s>0}} \ell_{\mathrm{type},j} \cdot \left[\frac{g_{s,\mathrm{type},j}\, g_{b,\mathrm{type},j} \left(C_{c,\mathrm{type},j} - C_{a,j} \right)}{g_{s,\mathrm{type},j} + g_{b,\mathrm{type},j} + g_{s,\mathrm{type},j} g_{b,\mathrm{type},j} r_{m,\mathrm{type},j}} \right] \Delta z_j. \tag{C4}$$

[100] Assuming that turbulence yields to well-mixed conditions we replace $C_{a,j}$ in equation (C4) by C_a. Then the identification of the terms in C_a in equations (C4) and (8) leads to an expression for the bulk mesophyll resistance r_m in terms of leaf variables.

[101] **Acknowledgments.** The senior author was supported by a postdoctoral fellowship from the CNRS. This work was supported by the French programs AGRIGES and PNRH jointly founded by the BRGM, CEMAGREF, INRA, INSU/CNRS, IRD, and Météo-France. The authors wish to acknowledge the contributions made by Bernard Ladouche and Antoine Millet to the experimental setup and the isotopic sampling.

References

Aubinet, M., et al., Estimates of the annual net carbon and water exchange of forests: The EUROFLUX methodology, *Adv. Ecol. Res.*, *30*, 113–175, 2000.

Bakwin, P. S., et al., Determination of the isotopic ($^{13}C/^{12}C$) discrimination by terrestrial biology from a global network of observations, *Global Biogeochem. Cycles*, *12*, 555–562, 1998.

Baldocchi, D. D., and P. C. Harley, Scaling carbon dioxide and water vapor exchange from leaf to canopy in a deciduous forest, II, Model testing and application, *Plant Cell Environ.*, *18*, 1157–1173, 1995.

Baldocchi, D. D., et al., FLUXNET: A new tool to study the temporal and spatial variability of ecosystem-scale carbon dioxide, water vapor, and energy flux densities, *Bull. Am. Meteorol. Soc.*, *82*(11), 2415–2434, 2001.

Berbigier, P., J.-M. Bonnefond, and P. Mellmann, CO_2 and water vapour fluxes for 2 years above Euroflux forest site, *Agric. For. Meteorol.*, *108*, 183–197, 2001.

Bowling, D. R., P. P. Tans, and R. K. Monson, Partitioning net ecosystem carbon exchange with isotopic fluxes, *Global Change Biol.*, *7*, 127–145, 2001.

Brendel, O., Does bulk-needle $\delta^{13}C$ reflect short-term discrimination?, *Ann. For. Sci.*, *58*, 135–141, 2001.

Brooks, A., and G. D. Farquhar, Effect of temperature on the CO_2/O_2 specificity of ribulose-1,5-biphosphate carboxylase/oxygenase and the rate of respiration in the light, *Planta*, *165*, 397–406, 1985.

Buchmann, N., et al., Interseasonal comparison of CO_2 concentrations, isotopic composition and carbon dynamics in an Amazonian rainforest (French Guiana), *Oecologia*, *110*, 120–131, 1997.

Canadell, J. G., et al., Carbon metabolism of the terrestrial biosphere: A multitechnique approach for improved understanding, *Ecosystems*, *3*, 115–130, 2000.

Cellier, P., and Y. Brunet, Flux-gradient relationships above tall plant canopies, *Agric. For. Meteorol.*, *58*, 93–117, 1992.

Farquhar, G. D., and J. Lloyd, Carbon and oxygen isotope effects in the exchange of carbon dioxide between terrestrial plants and the atmosphere, in *Stable Isotopes and Plant Carbon-Water Relations*, edited by J. R. Ehleringer, A. E. Hall, and G. D. Farquhar, pp. 47–70, Academic, San Diego, Calif., 1993.

Farquhar, G. D., J. R. Ehleringer, and K. T. Hubick, Carbon isotope discrimination and photosynthesis, *Annu. Rev. Plant Physiol. Plant Mol. Biol.*, *40*, 503–537, 1989.

Finnigan, J. J., and M. R. Raupach, Transfer processes in plant canopies in relation to stomatal characteristics, in *Stomatal Function*, edited by E. Zeiger, G. D. Farquhar, and I. R. Cowan, pp. 385–429, Stanford Univ. Press, Stanford, Calif., 1987.

Goulden, M. L., et al., Measurements of carbon sequestration by long-term eddy-covariance: Methods and a critical evaluation of accuracy, *Global Change Biol.*, *2*, 169–182, 1996.

Granier, A., et al., The carbon balance of a young Beech forest, *Funct. Ecol.*, *14*, 312–325, 2000.

Jacobs, A. F. G., J. H. van Boxel, and R. H. Shaw, The dependance of canopy layer turbulence on within-canopy thermal stratification, *Agric. For. Meteorol.*, *58*, 247–256, 1992.

Janssens, I. A., et al., Productivity overshadows temperature in determining soil and ecosystem respiration across European forests, *Global Change Biol.*, *7*, 269–278, 2001.

Keeling, C. D., A mechanism for cyclic enrichment of carbon-12 in terrestrial plants, *Geochim. Cosmochim. Acta*, *24*, 299–313, 1961.

Lamaud, E., et al., The Landes experiment: Biosphere-atmosphere exchanges of ozone and aerosol particles, *J. Geophys. Res.*, *99*(D8), 16,511–16,521, 1994.

Lauteri, M., E. Brugnoli, and L. Spaccino, Carbon isotope discrimination in leaf soluble sugars and in whole-plant dry matter in *Helianthus annuus* L. grown under different water conditions, in *Stable Isotopes and Plant Carbon-Water Relations*, edited by J. R. Ehleringer, A. E. Hall, and G. D. Farquhar, pp. 93–108, Academic, San Diego, Calif., 1993.

Lavigne, M. B., et al., Comparing nocturnal eddy covariance measurements to estimates of ecosystem respiration made by scaling chamber measurements at six coniferous boreal sites, *J. Geophys. Res.*, *102*(D24), 28,977–28,985, 1997.

Leclerc, M. Y., and K. C. Beissner, The influence of atmospheric stability on the budgets of the Reynolds stress and turbulence kinetic energy

within and above a deciduous forest, *J. Appl. Meteorol.*, *29*, 916–933, 1990.

Le Roux, X., et al., Spatial distribution of leaf water-use efficiency and carbon isotope discrimination within an isolated tree crown, *Plant Cell Environ.*, *24*, 1021–1032, 2001.

Lin, G., and J. R. Ehleringer, Carbon isotopic fractionation does not occur during dark respiration in C_3 and C_4 plants, *Plant Physiol.*, *114*, 391–394, 1997.

Loreto, F., et al., Estimation of mesophyll conductance to CO_2 flux by three different methods, *Plant Physiol.*, *98*, 1437–1443, 1992.

Loustau, D., and H. Cochard, Utilisation d'une chambre de transpiration portable pour l'estimation de l'évapotranspiration d'un sous-bois de pin maritime à molinie (*Molinia coerulea* (L) Moench), *Ann. Sci. For.*, *48*, 29–45, 1991.

Ogée, J., et al., MuSICA, a CO_2, water and energy multi-layer, multi-leaf pine forest model: Evaluation from hourly to yearly time scales and sensitivity analysis, *Global Change Biol.*, *9*(5), 697–717, 2003.

Porté, A., et al., Estimating the foliage area of maritime pine (*Pinus pinaster* Aït.) branches and crowns with application to modelling the foliage area distribution in the crown, *Ann. For. Sci.*, *57*, 73–86, 2000.

Press, W. H., S. A. Teukolski, W. T. Vettering, and B. P. Flannery, *Numerical Recipes in Fortran 77*, 2nd ed., 933 pp., Cambridge Univ. Press, New York, 1992.

Raupach, M. R., Applying Lagrangian fluid mechanics to infer scalar source distributions from concentration profiles in plant canopies, *Agric. For. Meteorol.*, *47*, 85–108, 1989a.

Raupach, M. R., A practical Lagrangian method for relating scalar concentrations to source distributions in vegetation canopies, *Q. J. R. Meteorol. Soc.*, *115*, 609–632, 1989b.

Raupach, M. R., Inferring biogeochemical sources and sinks from atmospheric concentrations: General consideration and application in vegetation canopies, in *Global Biogeochemical Cycles in the Climate System*, edited by E. D. Schultze et al., pp. 41–60, Academic, San Diego, Calif., 2001.

Running, S. W., et al., A global terrestrial monitoring network integrating tower fluxes, flask sampling, ecosystem modeling and EOS satellite data, *Remote Sens. Environ.*, *70*, 108–127, 1999.

Shaw, R. H., G. den Hartog, and H. H. Neumann, Influence of foliar density and thermal stability on profiles of Reynolds stress and turbulence intensity in a deciduous forest, *Boundary Layer Meteorol.*, *45*, 391–409, 1988.

Valentini, R., et al., Respiration as the main determinant of carbon balance in European forests, *Nature*, *404*, 861–865, 2000.

Villar, R., A. A. Held, and J. Merino, Dark leaf respiration in light and darkness of an evergreen and a deciduous plant species, *Plant Physiol.*, *107*, 421–427, 1995.

Warland, J. S., and G. W. Thurtell, A Lagrangian solution to the relationship between a distributed source and concentration profile, *Boundary Layer Meteorol.*, *96*, 453–471, 2000.

Yakir, D., and X.-F. Wang, Fluxes of CO_2 and water between terrestrial vegetation and the atmosphere estimated from isotope measurements, *Nature*, *380*, 515–517, 1996.

G. Bardoux, T. Bariac, P. Peylin, P. Richard, and C. Roche, LBI, CNRS-INRA-UPMC, Paris, France. (bardoux@grignon.inra.fr; Thierry.Bariac@grignon.inra.fr; peylin@lsce.saclay.cea.fr; Patricia.Richard@grignon.inra.fr; roche@ccr.jussieu.fr)

P. Berbigier, J.-M. Bonnefond, and Y. Brunet, Bioclimatologie, INRA-Bordeaux, Villenave d'Ornon, France. (Paul.Berbigier@bordeaux.inra.fr; bonnefond@bordeaux.inra.fr; Yves.Brunet@bordeaux.inra.fr)

P. Ciais and J. Ogée, Laboratoire des Sciences du Climat et de l'Environnement, UMR-CEA/CNRS, Bat. 709, Orme des Merisiers, F-91191 Gif/Yvette Cedex, France. (ciais@lsce.saclay.cea.fr; ogee@lsce.saclay.cea.fr)